Magnetoresitive sensors: steps towards the perfect sensor

Susana Cardoso de Freitas

INESC – Microsystems and Nanotechnologies
Lisbon, Portugal
www.inesc-mn.pt

Developing path of magnetic sensing technology

Hall Sensor → AMR → GMR → TMR

Spinvalve

Hall effect	AMR effect	GMR effect	TMR effect
0.2 ~ 0.8 mV/V/Gs	0.1 ~ 0.3 mV/V/Gs	0.2 ~ 1 mV/V/Gs	2 ~ 10 mV/V/Gs

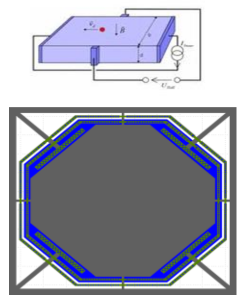

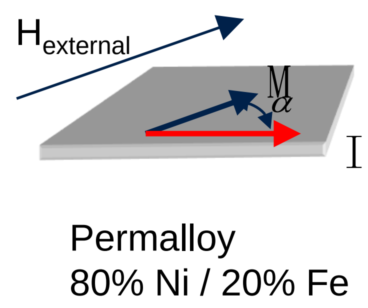

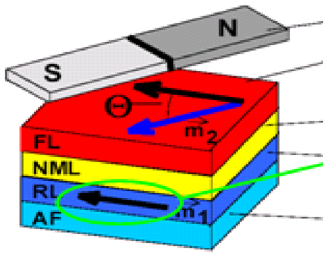

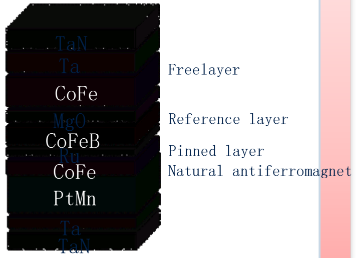

Hard Disks 1986 → 1996 → 2004 →

SENSORS Hall → AMR → GMR → TMR →

The perfect magnetoresistive sensor

IEEE Trans Magn. 53 (4), 5300204 (2017

- large output voltage:	mV
- low field detection:	pT
- tunable for large field detection:	80 mT
- low noise	
- low hysteresis	0 mT
- linearity:	< 1% non-linearity
- small footprint:	10 µm chip size
- low cost:	< 0.20 €/chip
- high thermal stability:	>120°C in harsh e.m environment

- compatible with CMOS modules
- compatible with large scale microfabrication
- compatible with flexible electronics

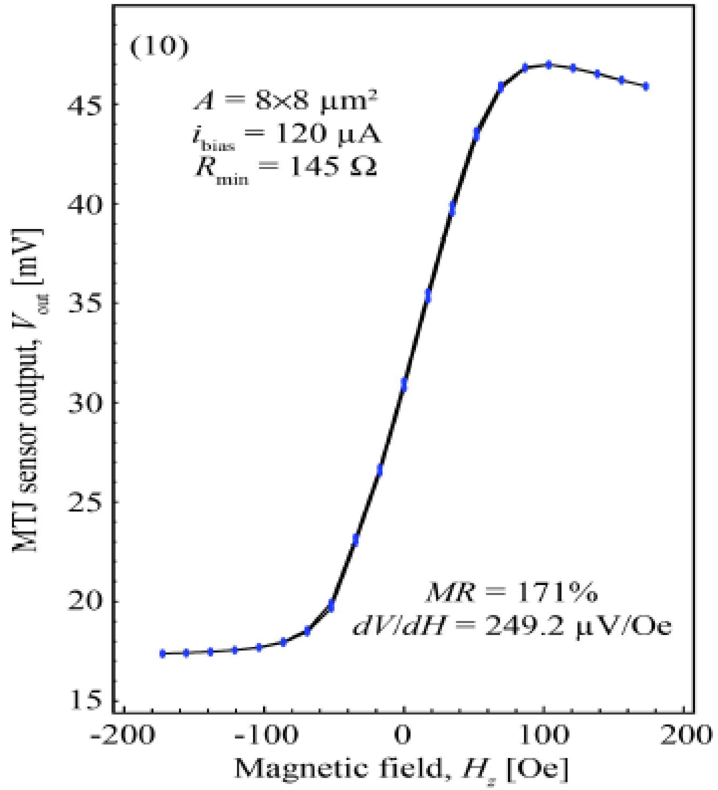

Magnetoresistive sensors

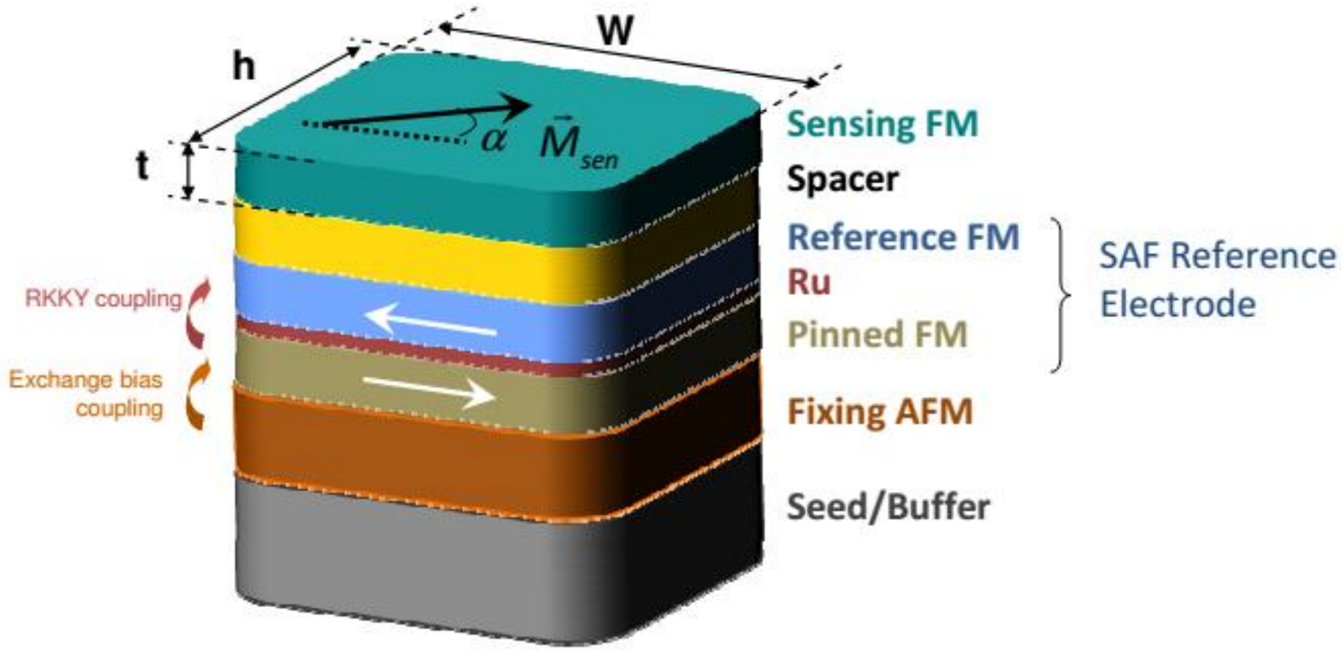

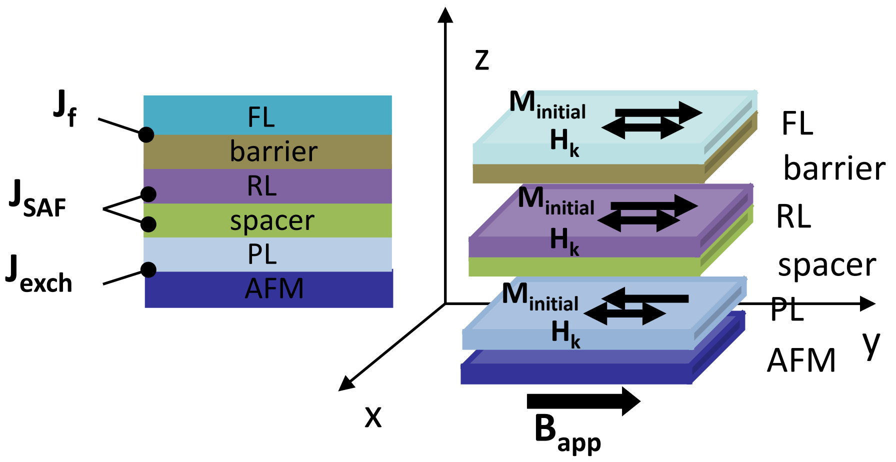

TMR sensor with AlOx barrier (2001)

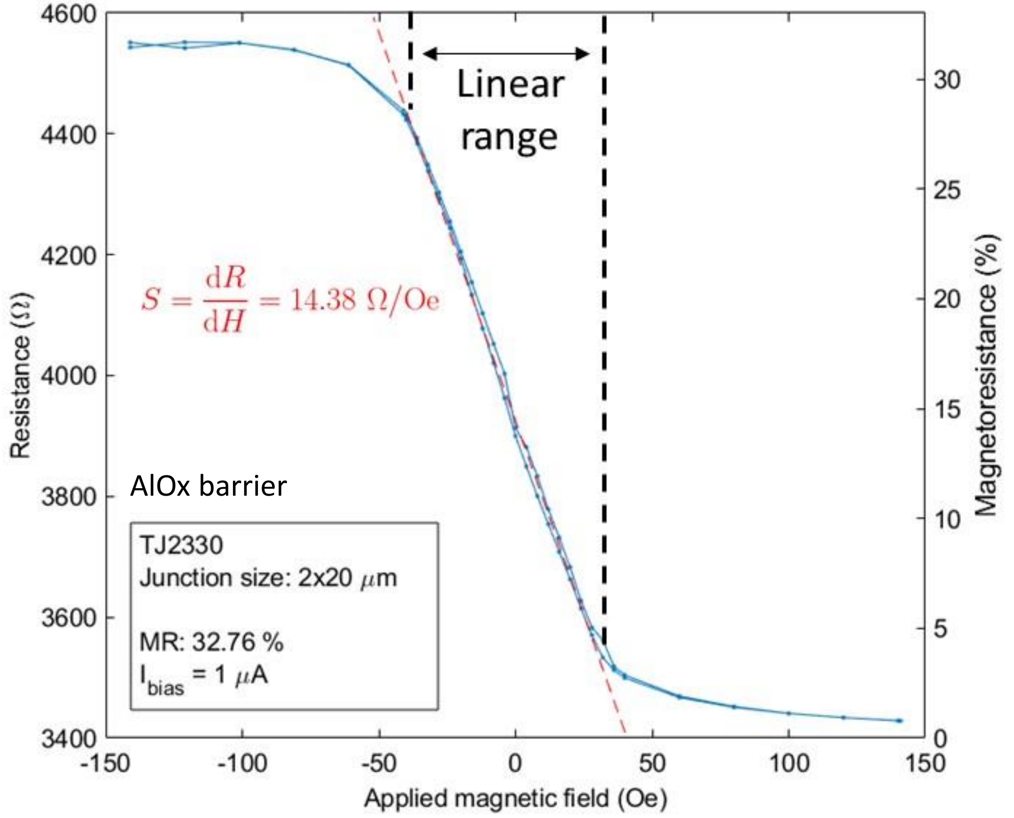

Magnetic tunnel junction - TMR

INESC MN
Microsistemas & Nanotecnologias

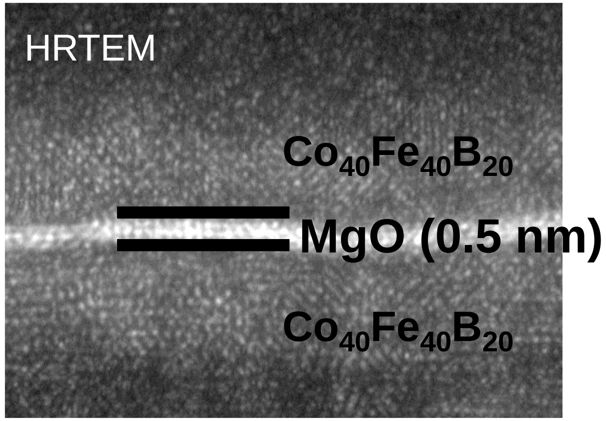

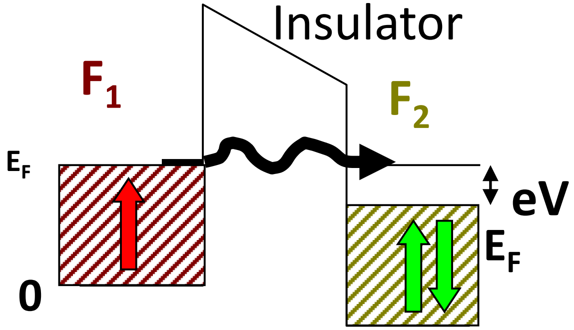

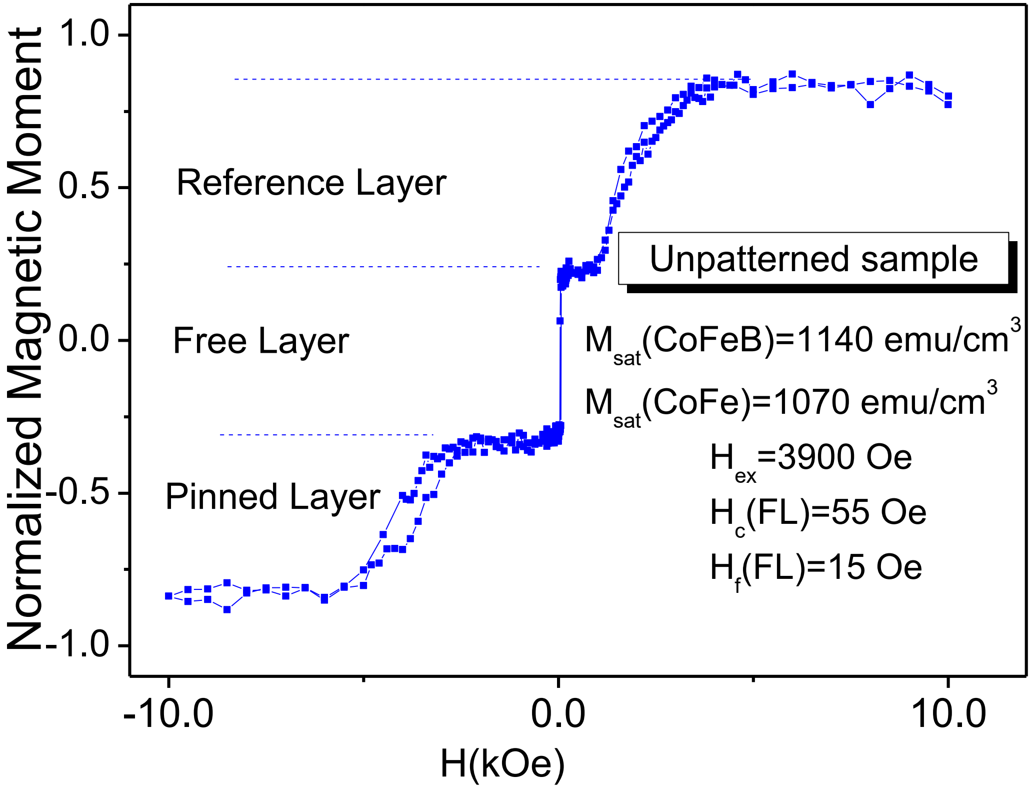

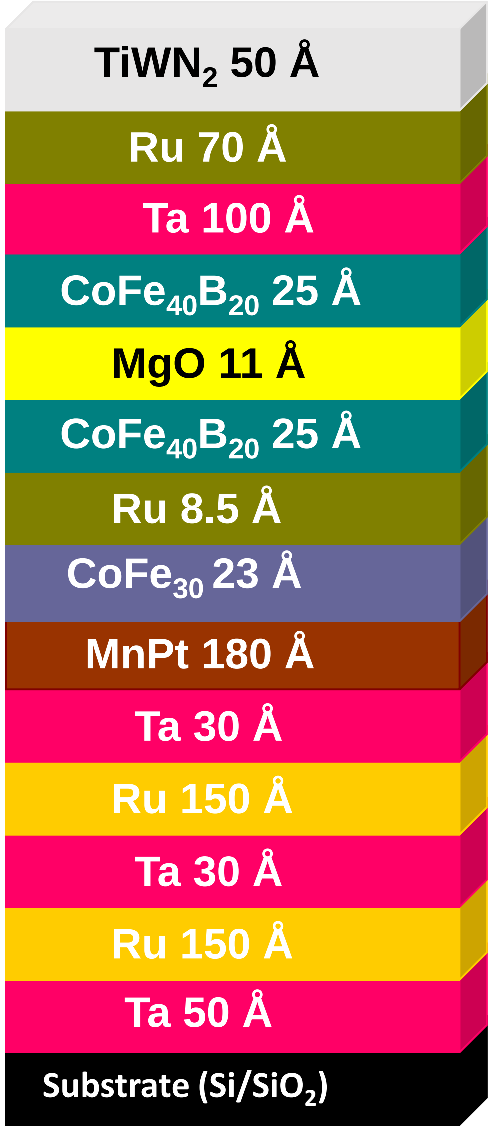

MIT, 1996
IBM, 1997
INESC, 1997

Electrons will tunnel if apply voltage between electrodes
Spin is conserved upon tunneling

AlOx and MgO barriers

INESC MN
Microsistemas & Nanotecnologias

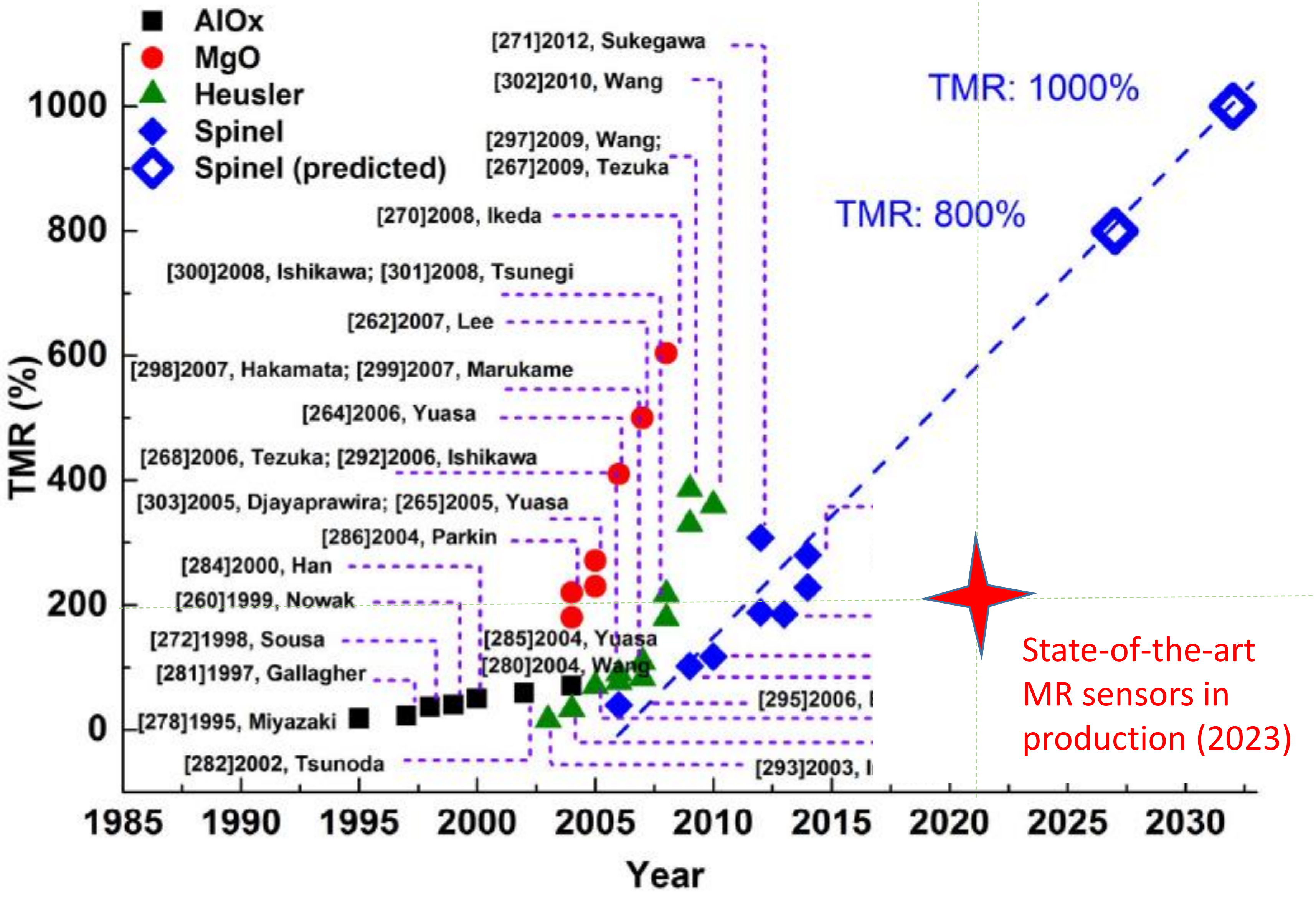

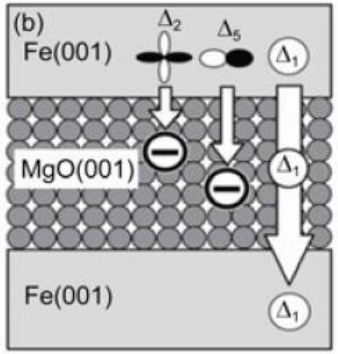

Crystalline barrier

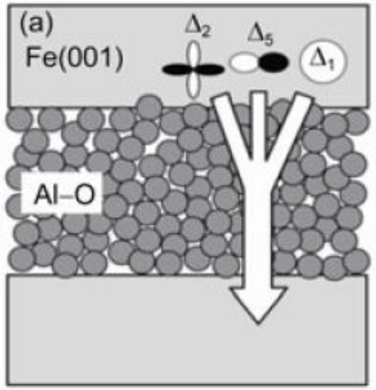

Amorphous barrier

"Magnetoresistive Sensor Development Roadmap (Non-Recording Applications)"
IEEE Trans.Magn. (2019)

Micromagnetic and Analytical Models

INESC MN
Microsistemas & Nanotecnologias

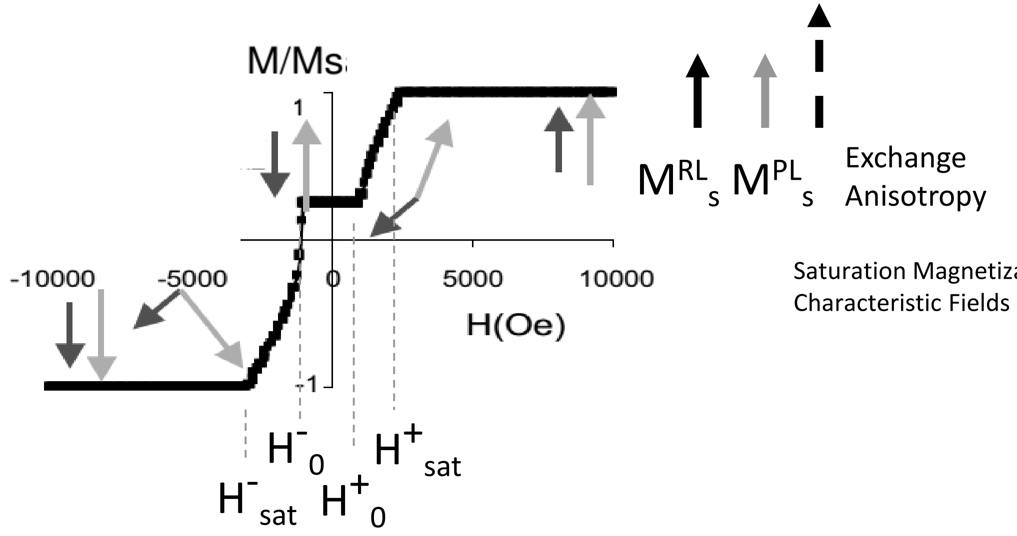

Saturation Magnetizations (M^s)
Characteristic Fields (H_{sat}, H_o)

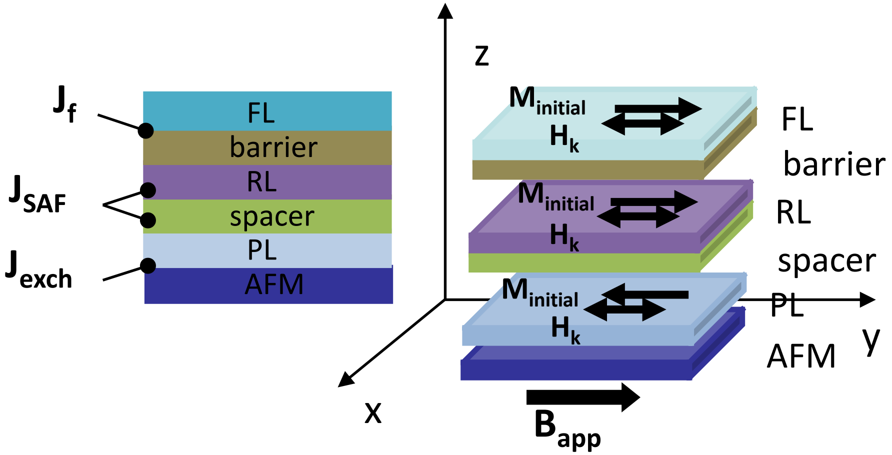

Nanotechnology 27, 045501 (2015)

Magnetoelectronics, Elsevier, Ed. Mark Jonhson, 2004

Experimental

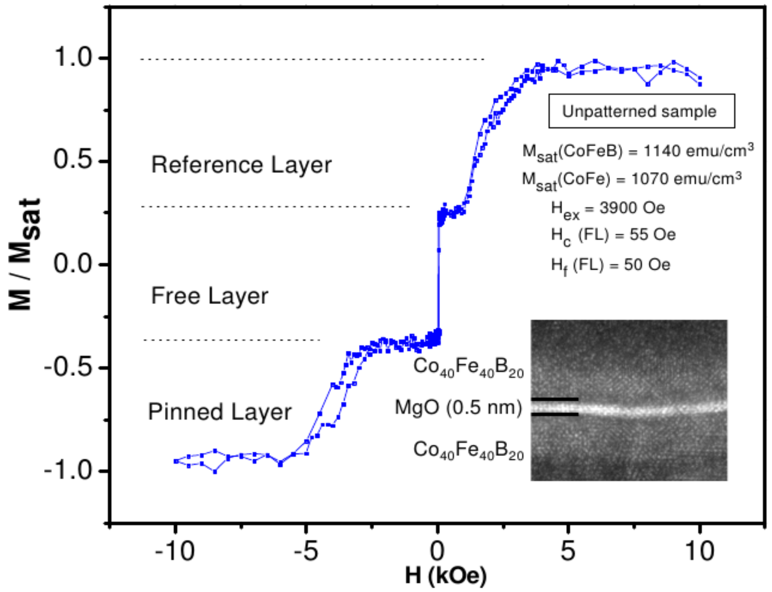

M_{sat}

J_{exch}
J_{SAF}
Jf

Simulation

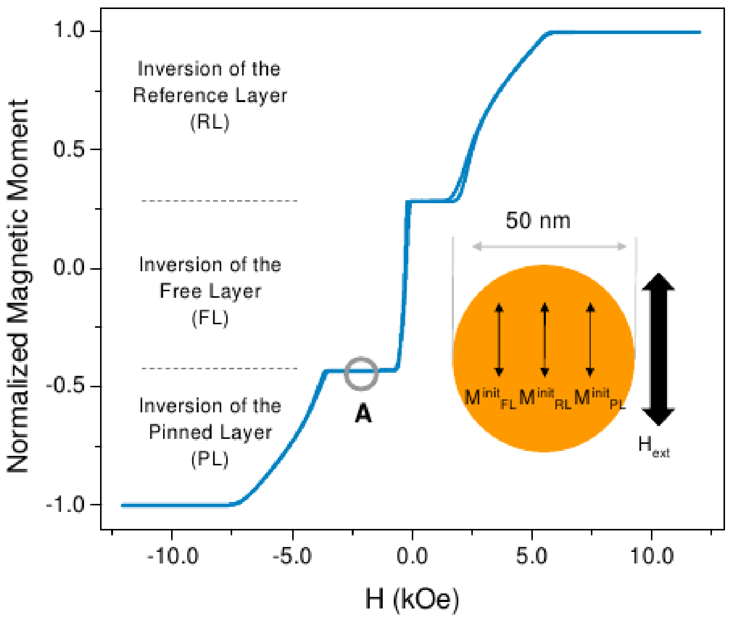

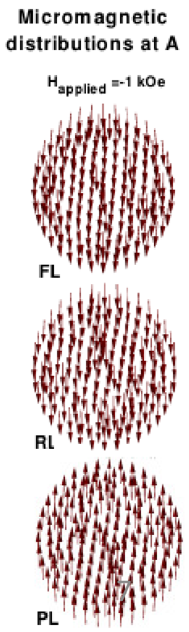

INESC MN
Microsistemas & Nanotecnologias

Magnetic Energy of a semi-infinite thin film **(w>>h,t)**

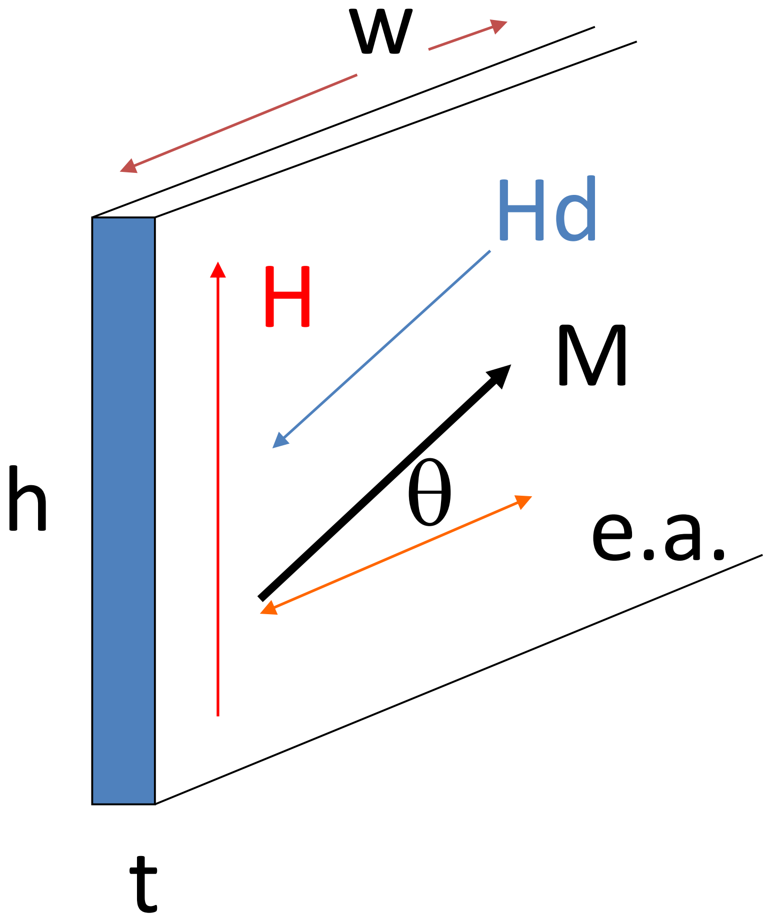

$$E/V = -\mu_o H.M + K \sin^2\theta - ½ \mu_o H_d.M$$

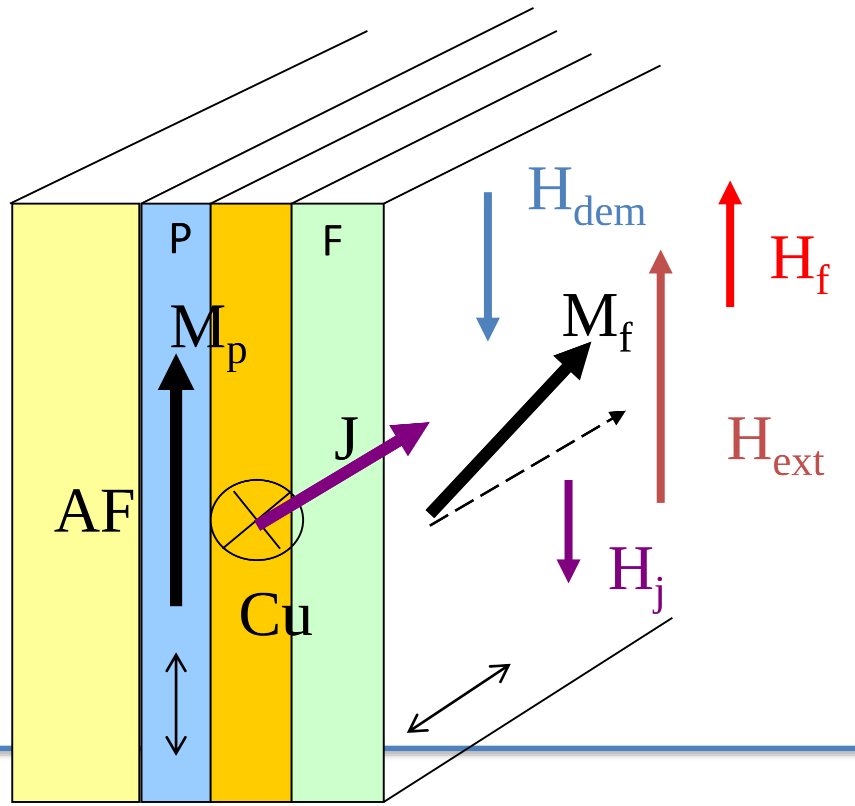

Theory Magnetic Recording, N.Bertram
B.D.Cullity(1972) Introduction to Magnetic Materials
1- C.Tsang, et.al, IEEE Trans.Magn., 30, 3801 (1994).
2- B.Dieny, et.al Phys.Rev.B, 43, 1297(1991).
3- D.E.Heim, et.al , IEEE Trans.Magn.., 30, 316 (1994);
4- P.P.Freitas, et.al , Appl.Phys.Lett., 65, 493 (1994);

Modelling - micromagnetics

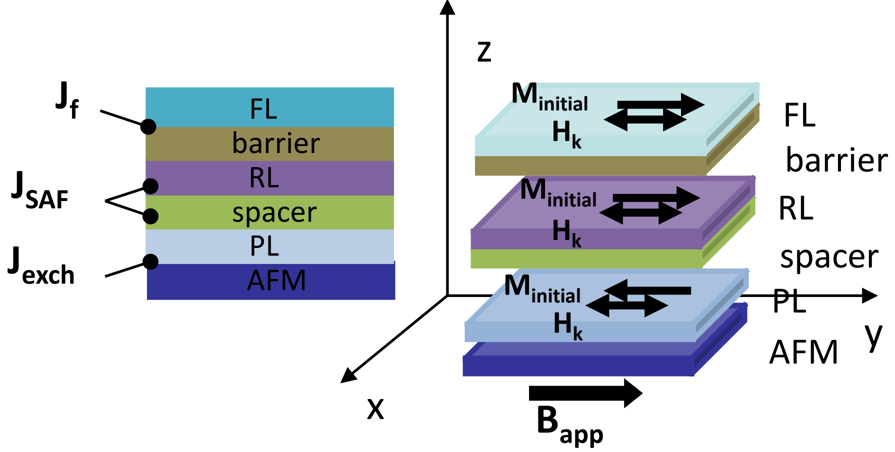

Magnetic volumic properties		
for all ferromagnetic volumes		
Saturation flux densities µ0Ms	***T***	***Initial M versor***
Uniaxial anisotropy flux density Hk	***T***	***Anisotropy versor***
for all micromagnetic volumes		
Surface Energy Coupling constants (erg/cm²)		
Allmicromagnetic surfaces		
Exchange coupling between PL and AFM	**J_{exch}**	
Néel Ferromagnetix Coupling	**J_f**	
AntiFerromagnetic coupling trough spacer	**J_{SAF}**	

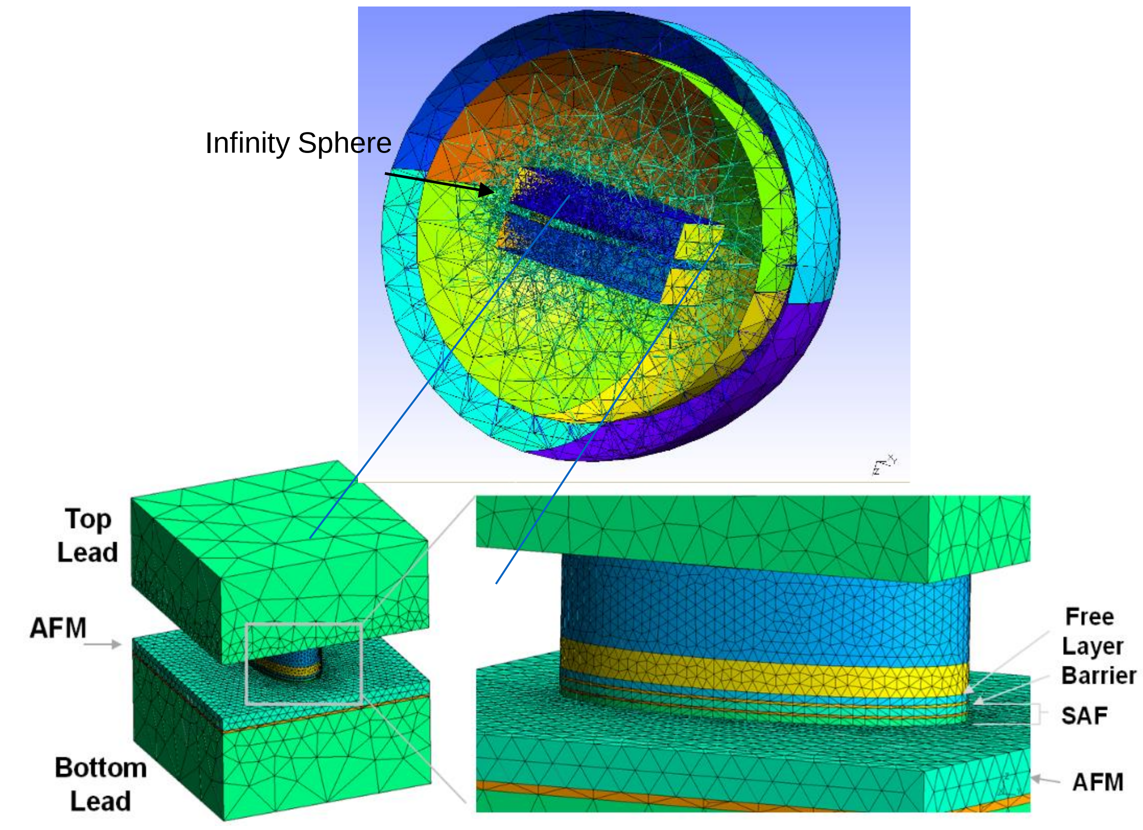

Macrospin Model for MR sensors

INESC MN
Microsistemas & Nanotecnologias

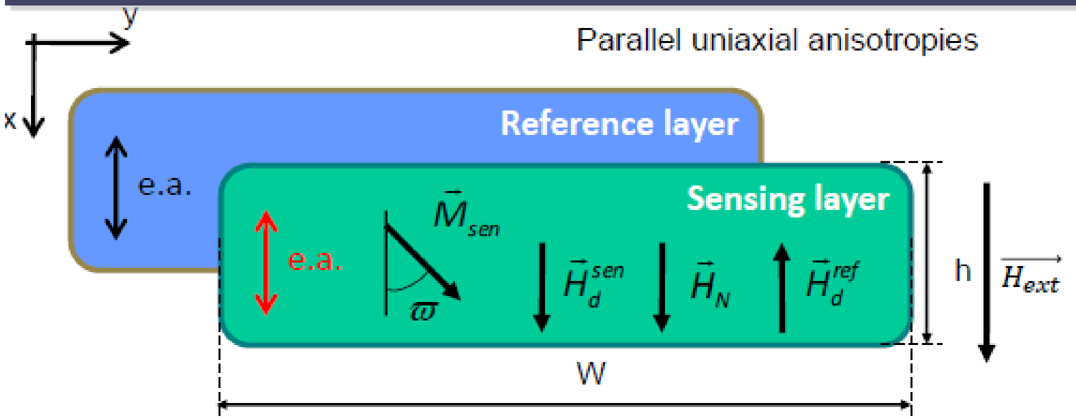

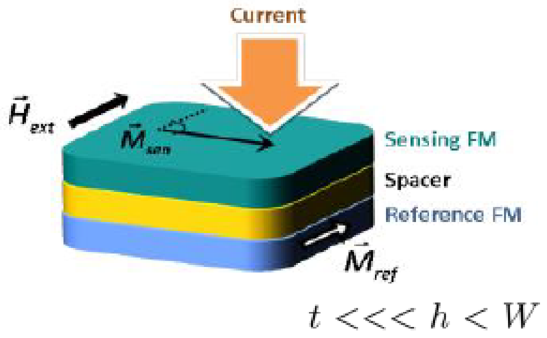

Energy minimization

When $H_{ap} < H^{ref}{}_d - H_N - |H_k - N_h M^{sen}{}_s|$

Minimum @ $\varpi = \pi$

When $H_{ap} > H^{ref}{}_d - H_N + |H_k - N_h M^{sen}{}_s|$

Minimum @ $\varpi = 0$

When $|H_{ap} - H^{ref}{}_d + H_N| < |H_k - N_h M^{sen}{}_s|$

2 situations can occur:
If $H_k > N_h M^{sen}{}_s$

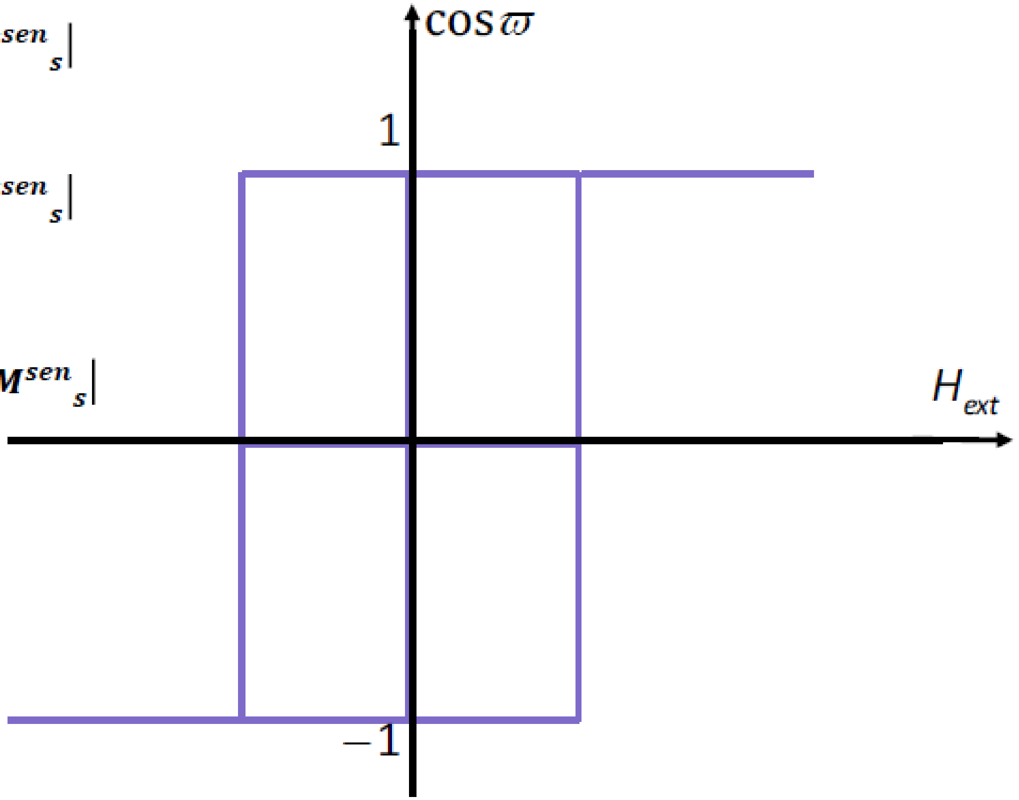

Macrospin Model for MR sensors

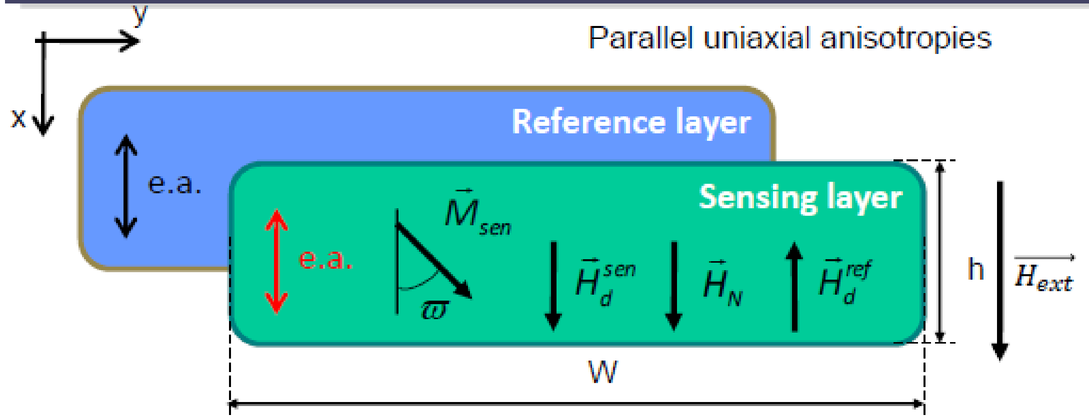

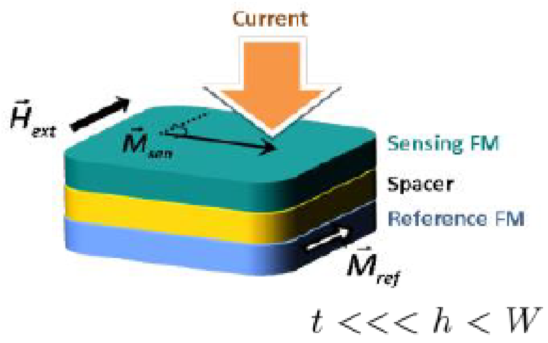

Energy minimization

When $H_{ap} < {H^{ref}}_d - H_N - |H_k - N_h {M^{sen}}_s|$

Minimum @ $\varpi = \pi$

When $H_{ap} > {H^{ref}}_d - H_N + |H_k - N_h {M^{sen}}_s|$

Minimum @ $\varpi = 0$

When $|H_{ap} - {H^{ref}}_d + H_N| < |H_k - N_h {M^{sen}}_s|$

2 situations can occur:

If $H_k < N_h {M^{sen}}_s$

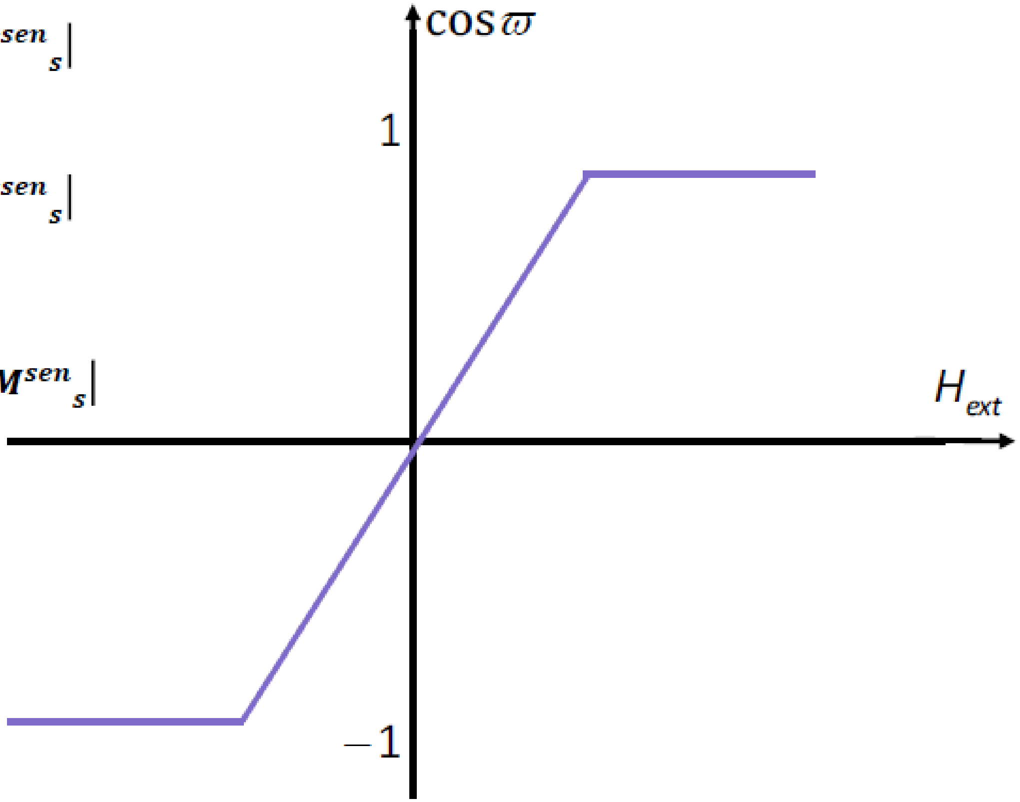

Macrospin Model for MR sensors

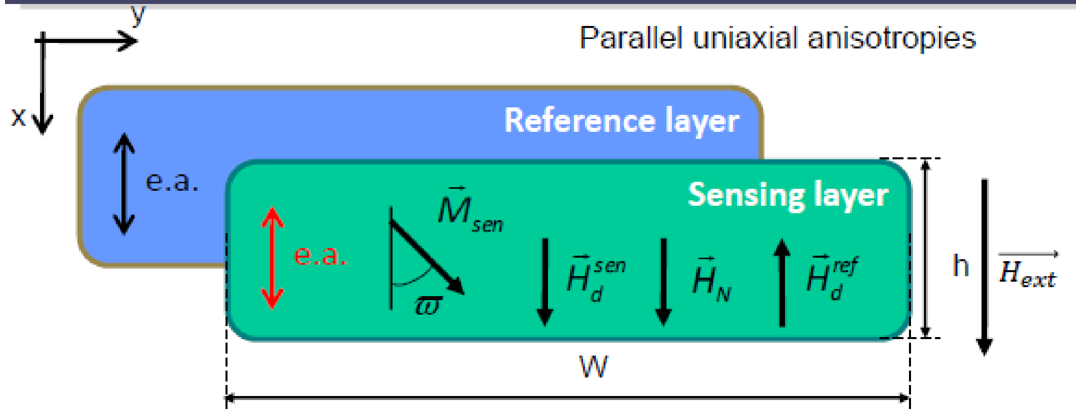

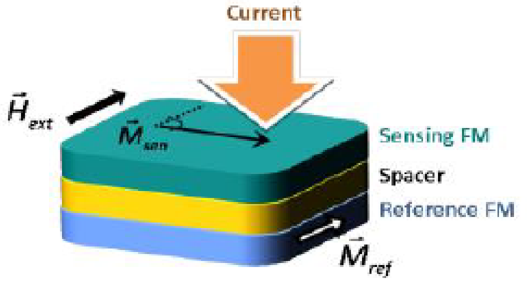

$t <<< h < W$

Final transfer curves

If $H_k > N_h M^{sen}_s$

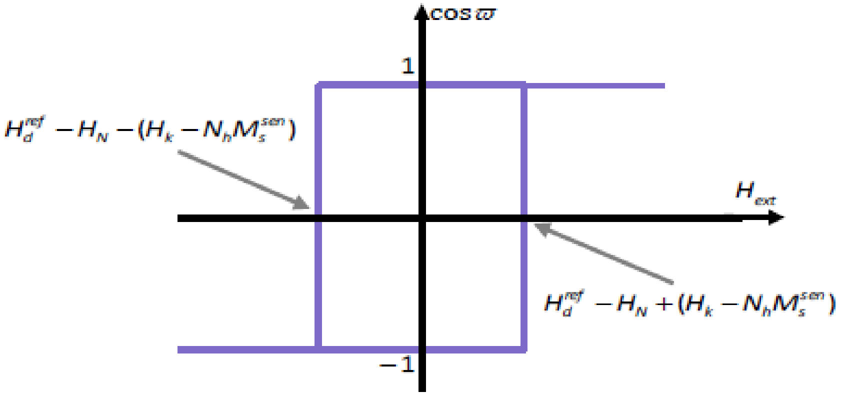

If $H_k < N_h M^{sen}_s$

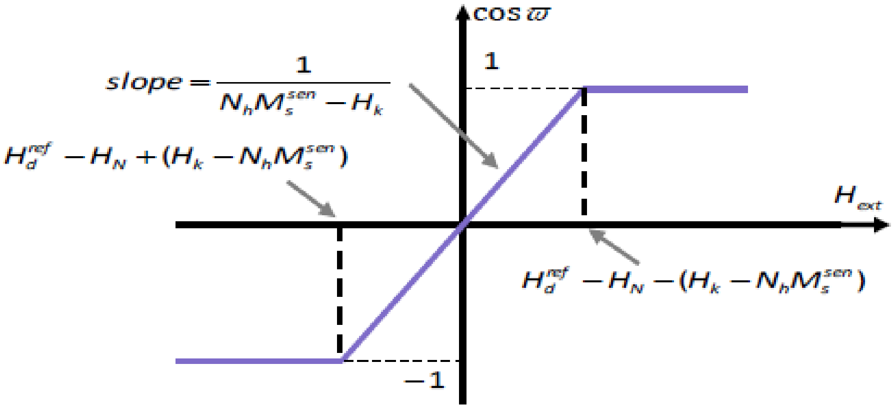

Memory applications:
Coercive field: $H_c = \frac{H_k - N_h M^{sen}_s}{2}$

Sensor applications:
Sensitivity $\propto$ *slope*
Highest sensitivity when $H_k = N_h M^{sen}_s$

Linearization strategies for MgO-MTJ

Magnetotransport curve:

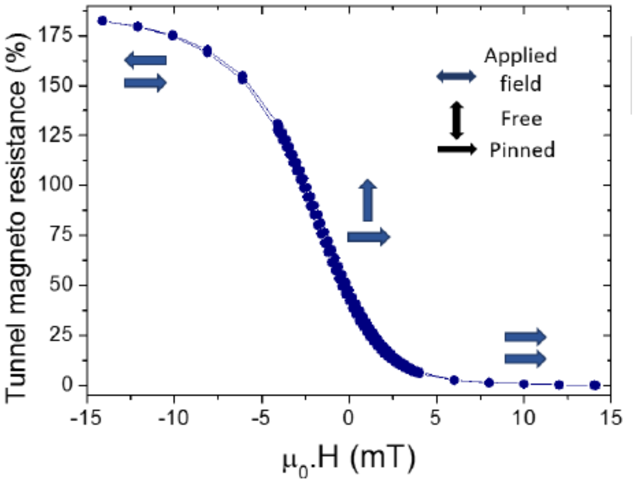

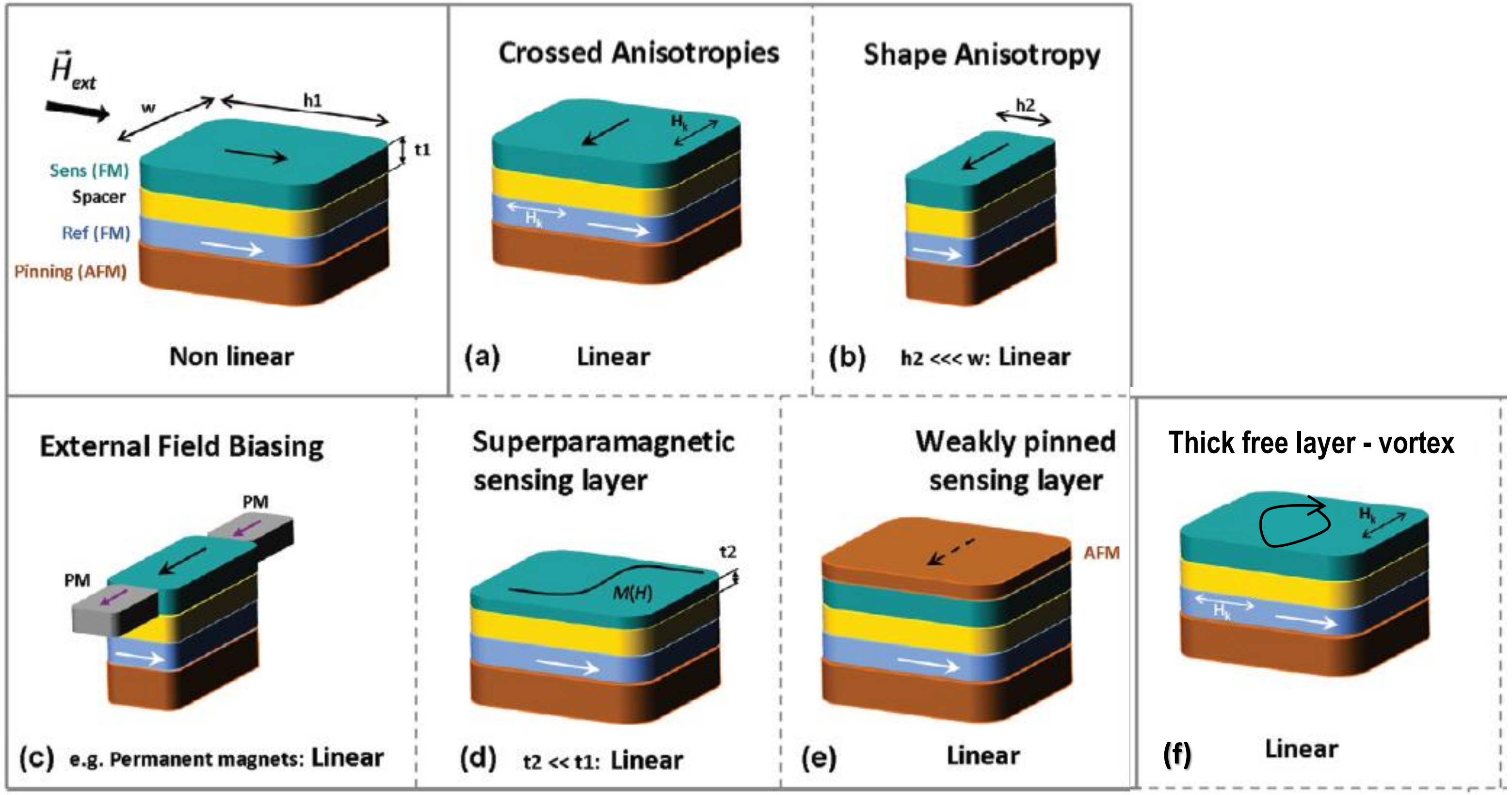

Fig. 12. Summary of linearization strategies for MR sensors.

J.Appl.Phys. 103, 07A910 (2008)
Sensors and Actuators , 202, pp. 64– 68 (2013);

Journal of SPIN, Vol.1 (1), pp 71-91 (2011)
*Silva et al. Eur. Phys. **J. Appl. Phys**. 72 (1) 10601 (2015)*

Suess, D., et al. Nat Electron 1, 362 (2018)

Eur. Phys. J. Appl. Phys. 72 (1) 10601 (2015)

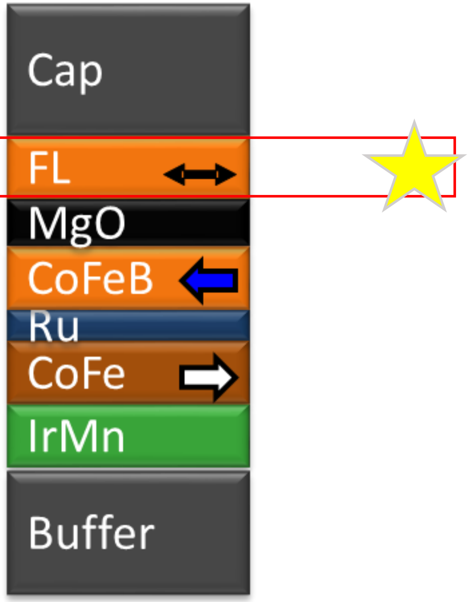

Shape anisotropy

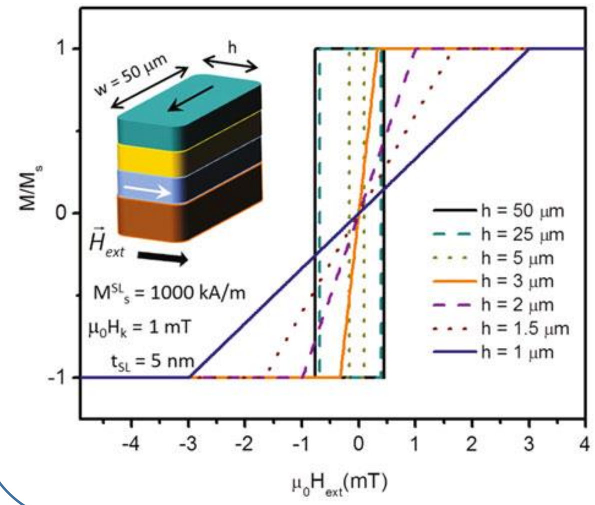

Weekly-pinned free layer

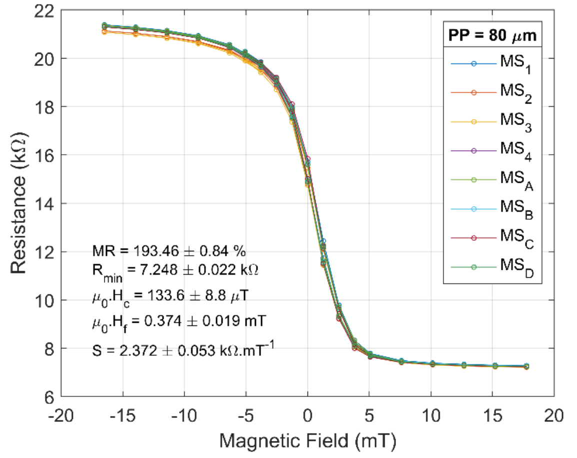

~ 1.8 – 6.0 nm (with linearization strategy)

Free layer thickness

<< 1.3 nm

~ 1.3 - 1.5 nm

> 30 nm

> 200mT linear range

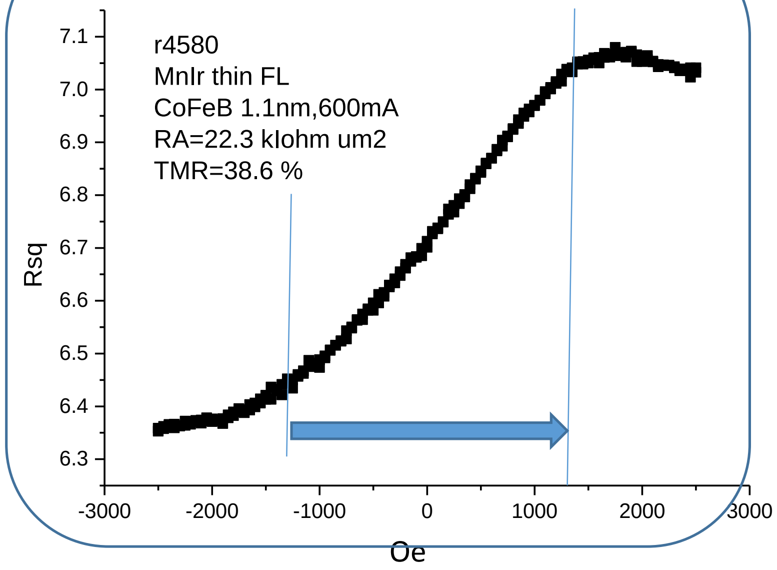

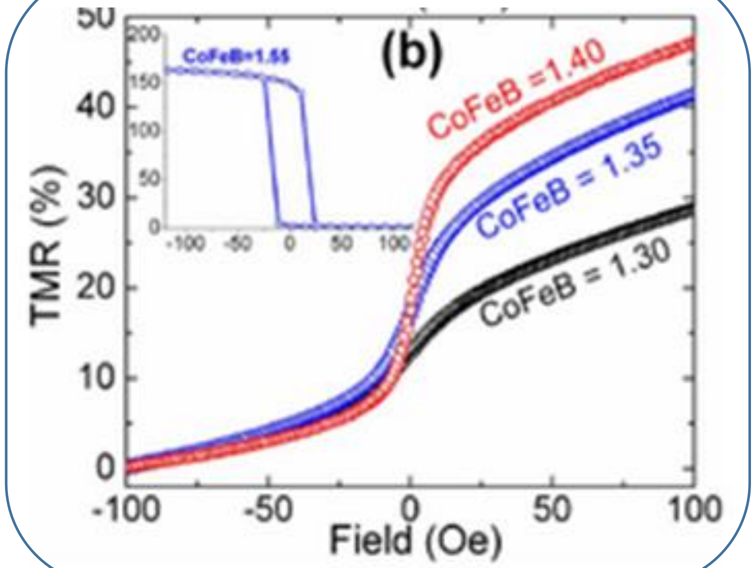

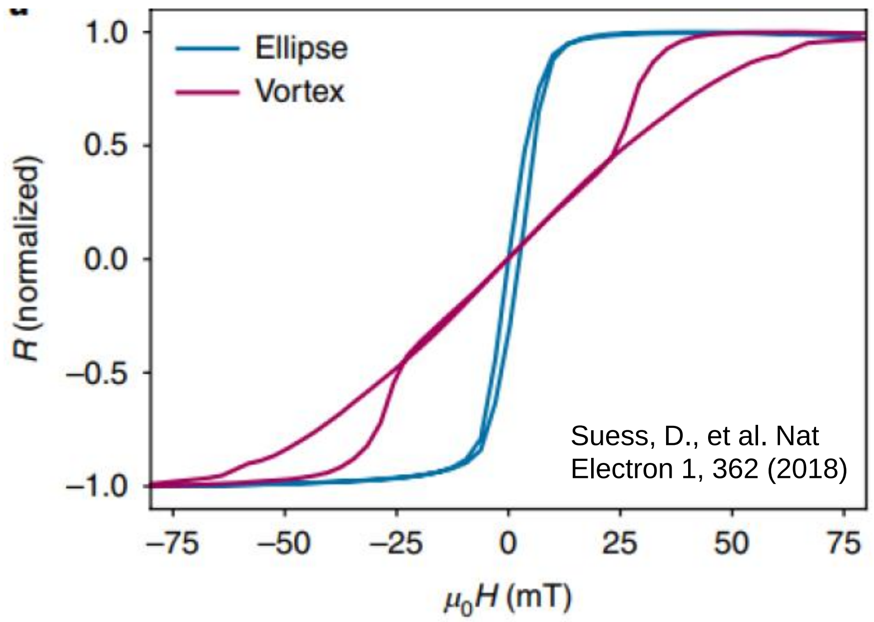

Suess, D., et al. Nat Electron 1, 362 (2018)

200mm backend GMR / TMR technology

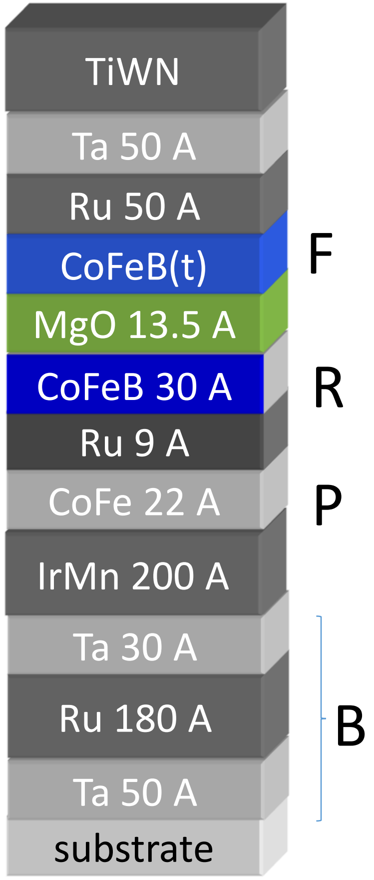

6 targets IBD (extra module 8 targets in PVD; 2019)
Dep pressure 2 x 10^{-5}Torr
Heated substrate
Assist gun,
Base Pressure $5x10^{-8}$ Torr

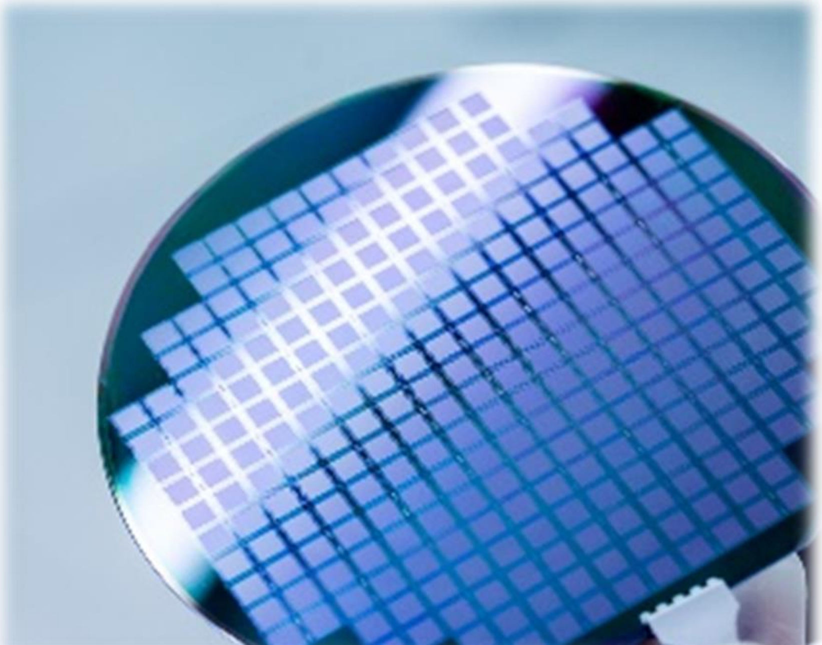

Nordiko
INNOVATION WITH RELIABILITY

Process control

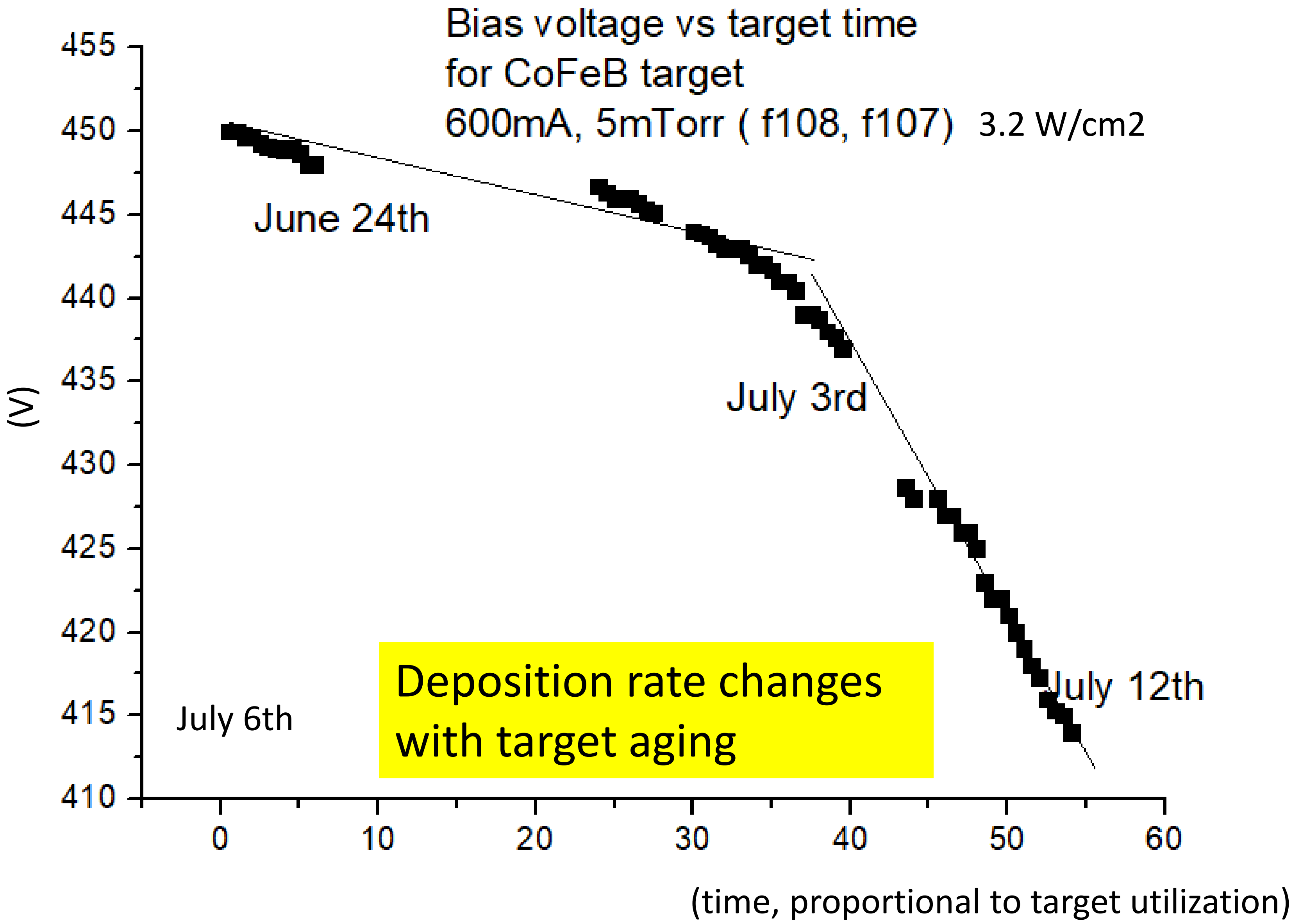

Deposition rate changes with target aging

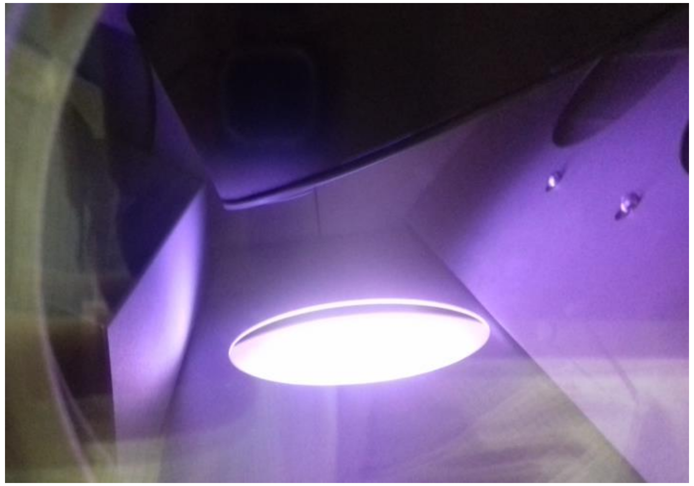

CoFeB sputtering target (Ø100mm)

Process control: free layer thickness

Stack:

[Ta 5/Ru 10]$_{x3}$/Ta 5/Ru 5/MnIr 8/CoFe 2.2/Ru 0.65/CoFeB 2/MgO 1.6/**CoFeB t**/Ta 5/Ru 5/Ta 5/Ru 10

5µm squares

< 0.1 nm
thickness accuracy
needed

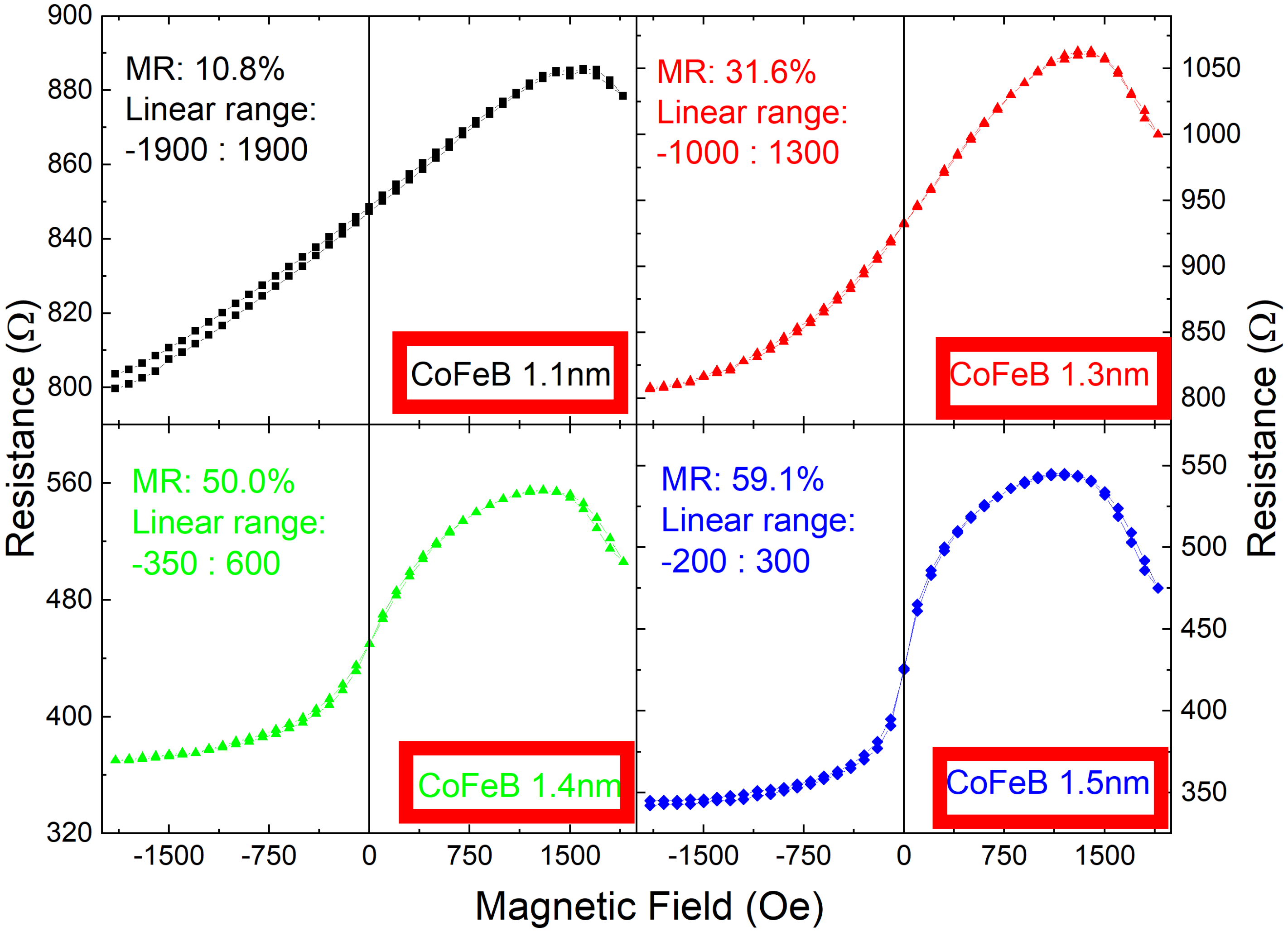

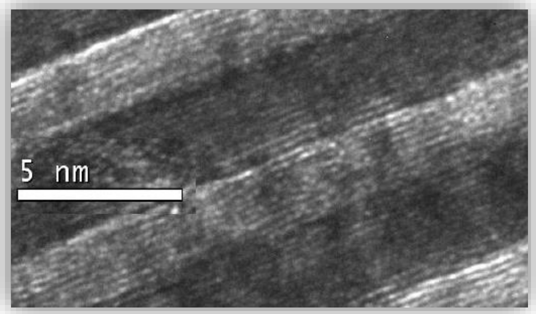

M.Caseiro

Process control: tunnel barrier thickness

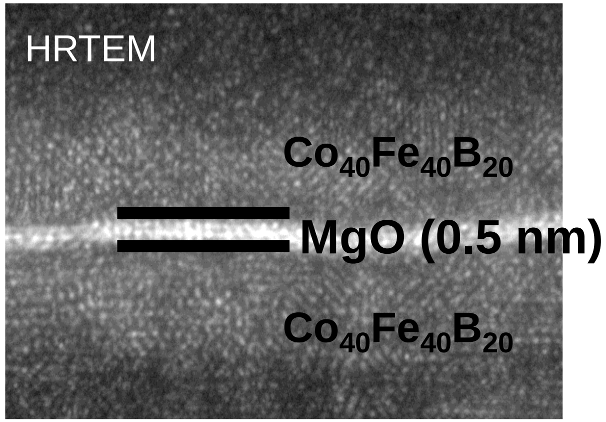

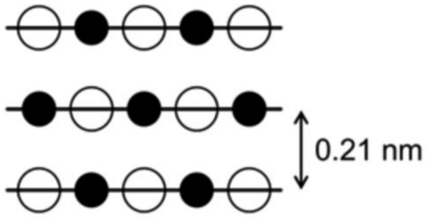

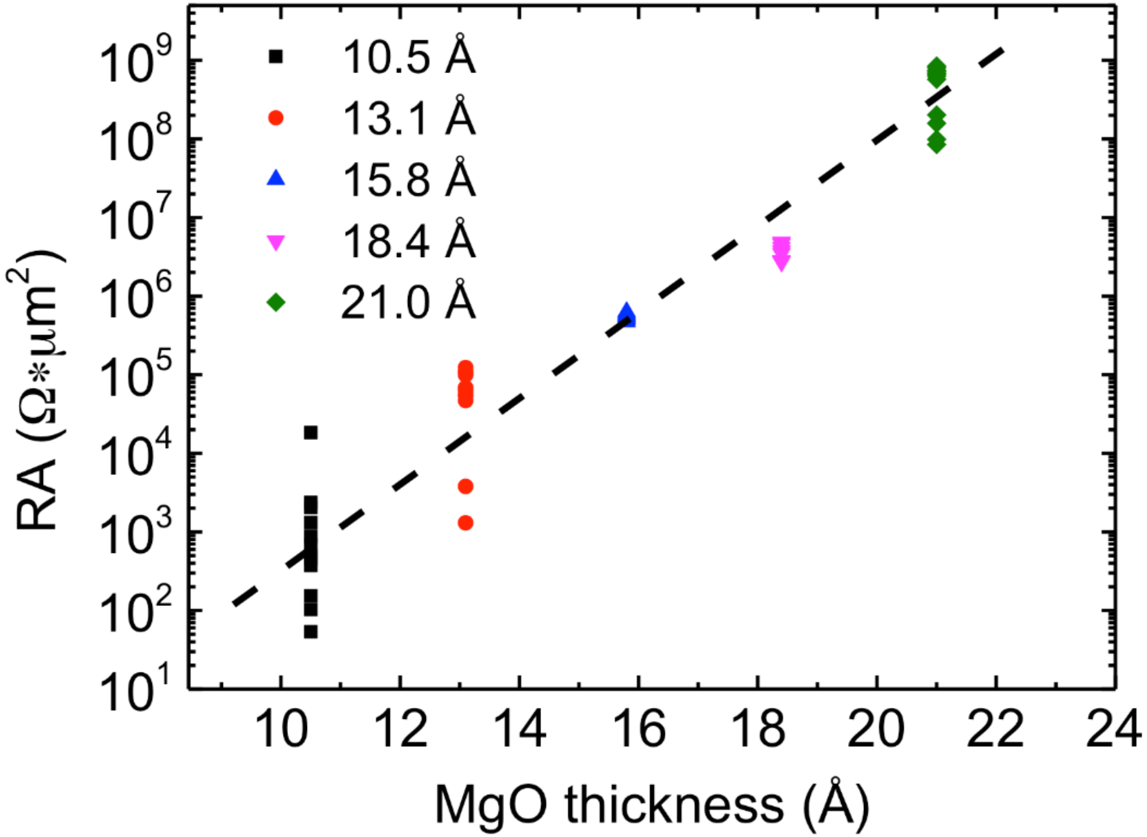

1 Å => 10x R

Interlayer magnetic coupling - Néel coupling

INESC MN
Microsistemas & Nanotecnologias

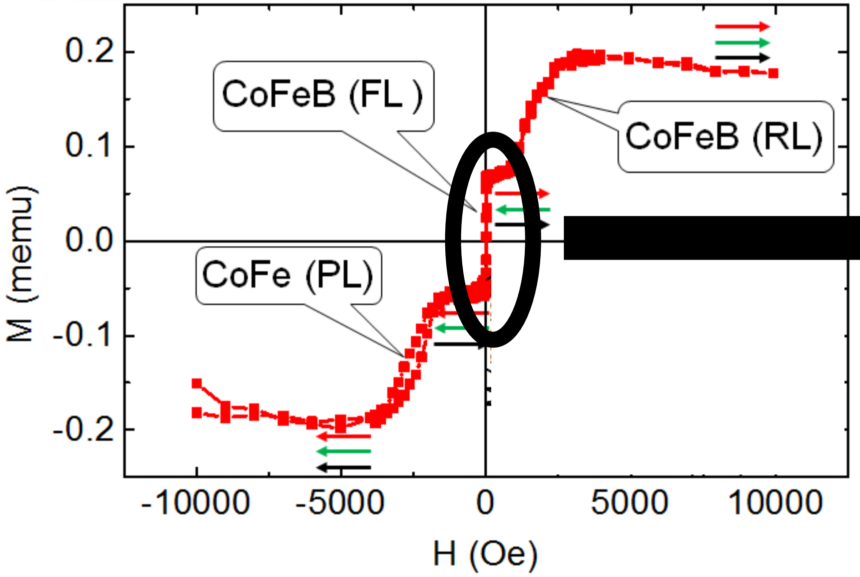

Looking near zero fields

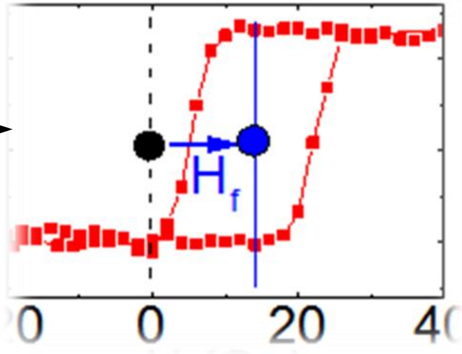

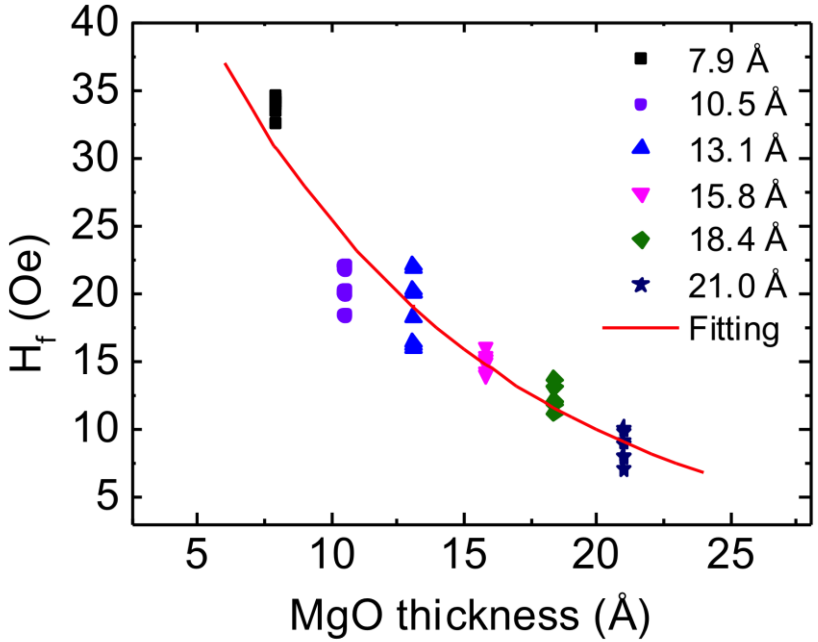

$$H_f = \frac{\pi^2 h^2 M_s}{\sqrt{2}\lambda t_{FL}} exp(-2\pi\frac{\sqrt{2}d}{\lambda}) \times [1 - exp(-2\pi\frac{\sqrt{2}t_{FL}}{\lambda})] \times [1 - exp(-2\pi\frac{\sqrt{2}t_{RL}}{\lambda})]$$

t_{FL} nm	t_{RL} nm	M_s emu/cc	λ nm	h nm
3	3	1466	9.47	0.13

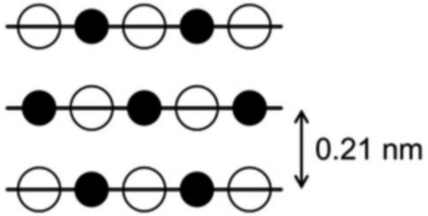

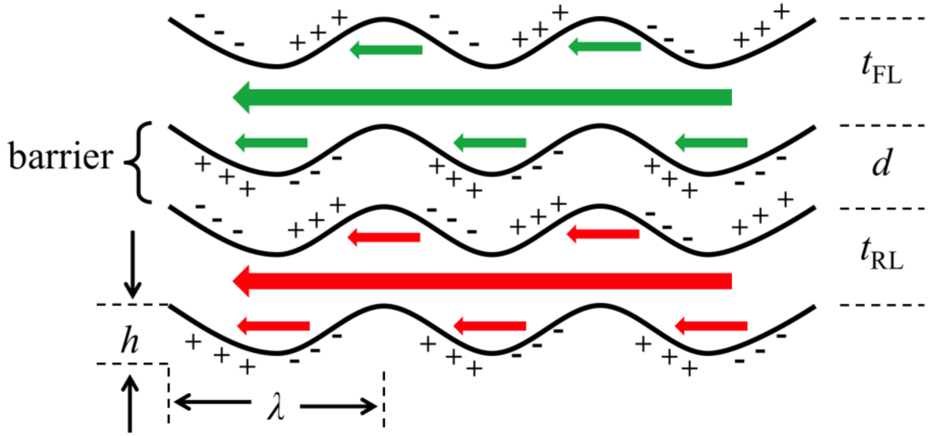

- A method to access the MgO/CoFeB roughness.

J. C. S. Kools, et.al., J. Appl. Phys. 85 , 4466 (1999).

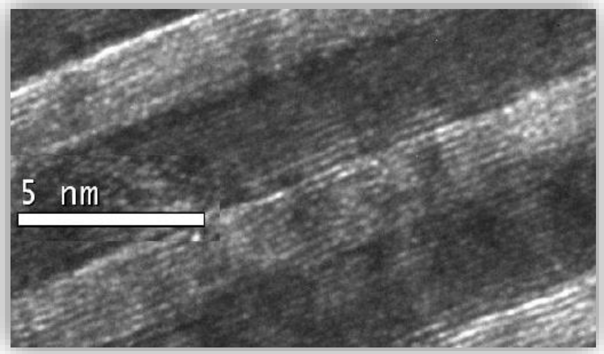

Film thickness:
Controlled at the atomic scale
1 Å = 0.1 nm

Multilevel device patterning

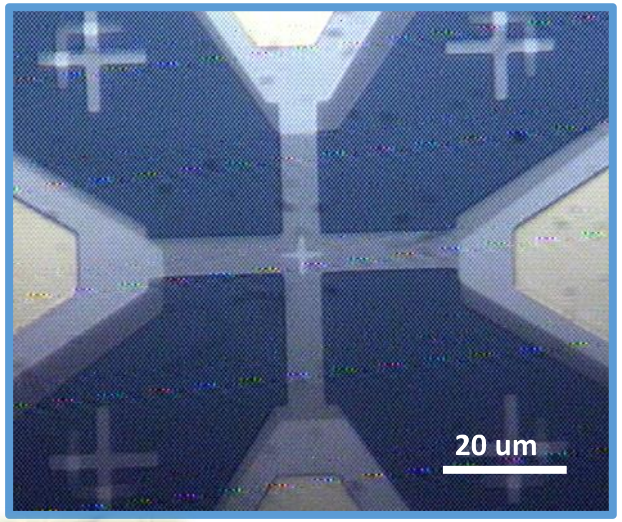

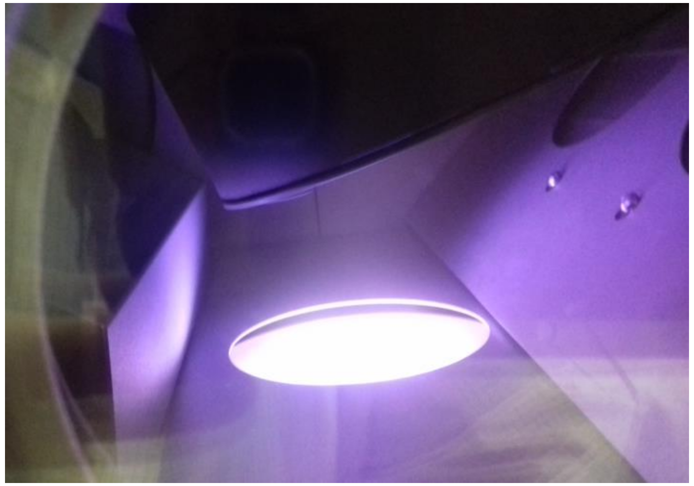

MgO target with Ar plasma

Wafer microfabrication in a Clean Room

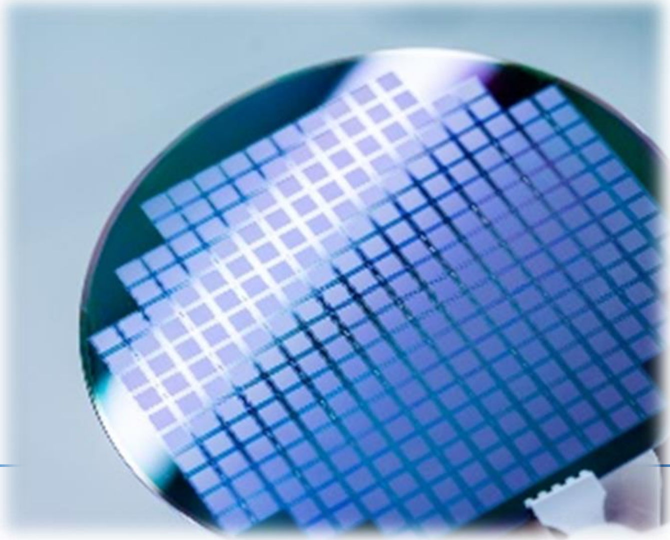

Current-perpendicular-to-plane (CPP) device fabrication

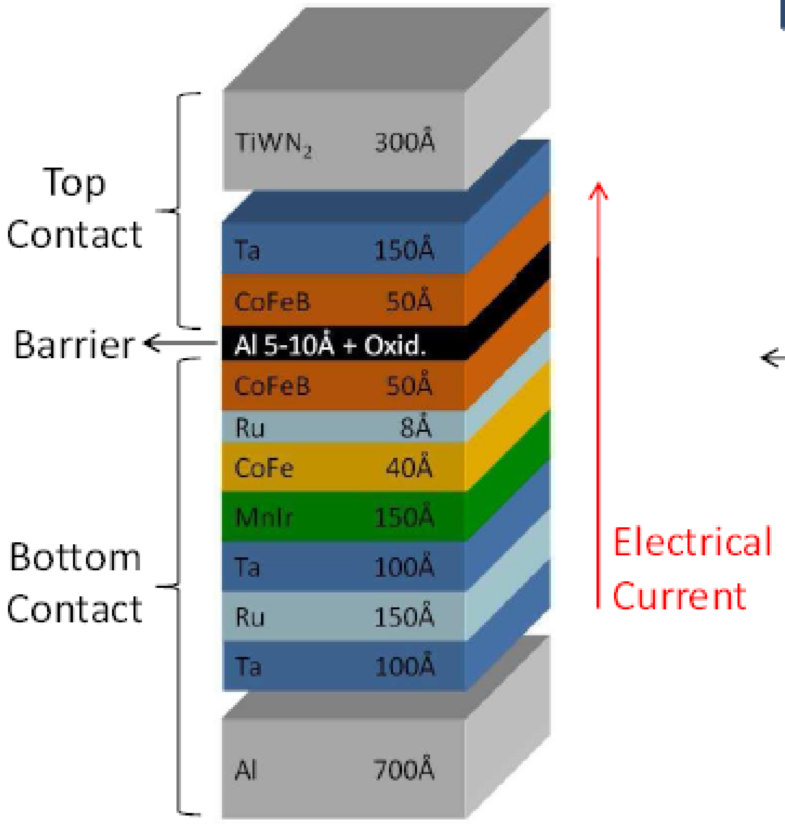

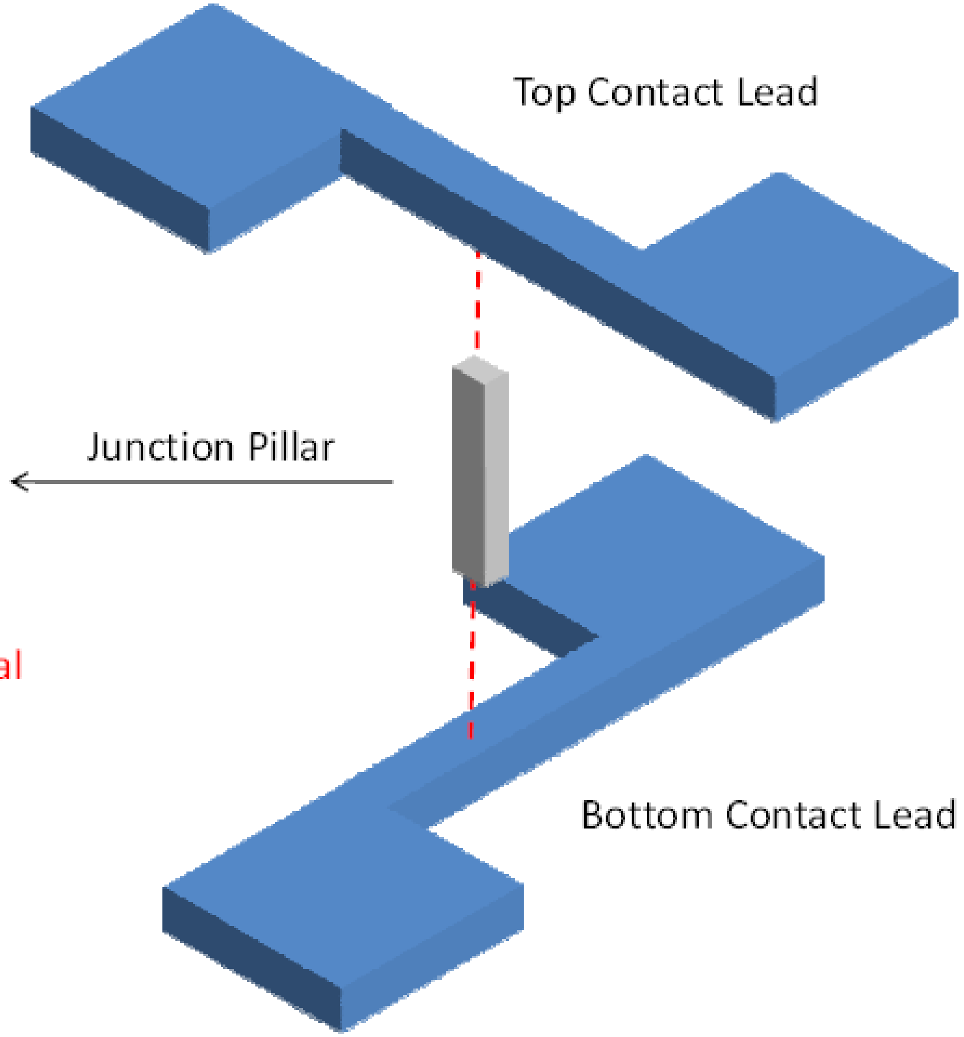

INESC MN
Microsistemas & Nanotecnologias

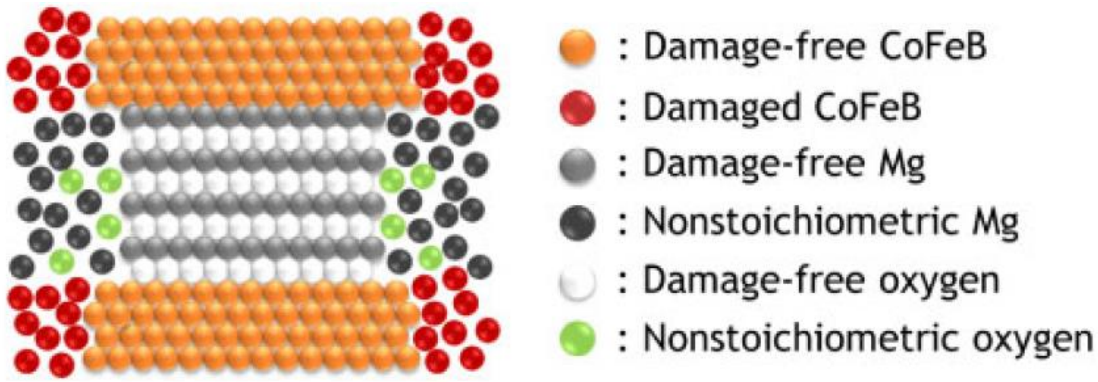

Fig. 5. (Color online) Substance distribution diagram of the patterned MTJs after the etching process.

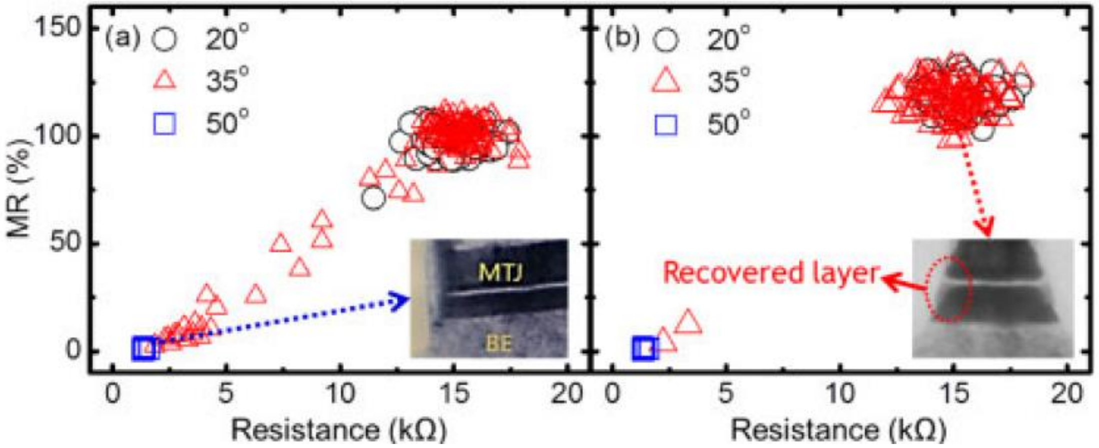

Japanese Journal of Applied Physics **56**, 04CE09 (2017)
https://doi.org/10.7567/JJAP.56.04CE09

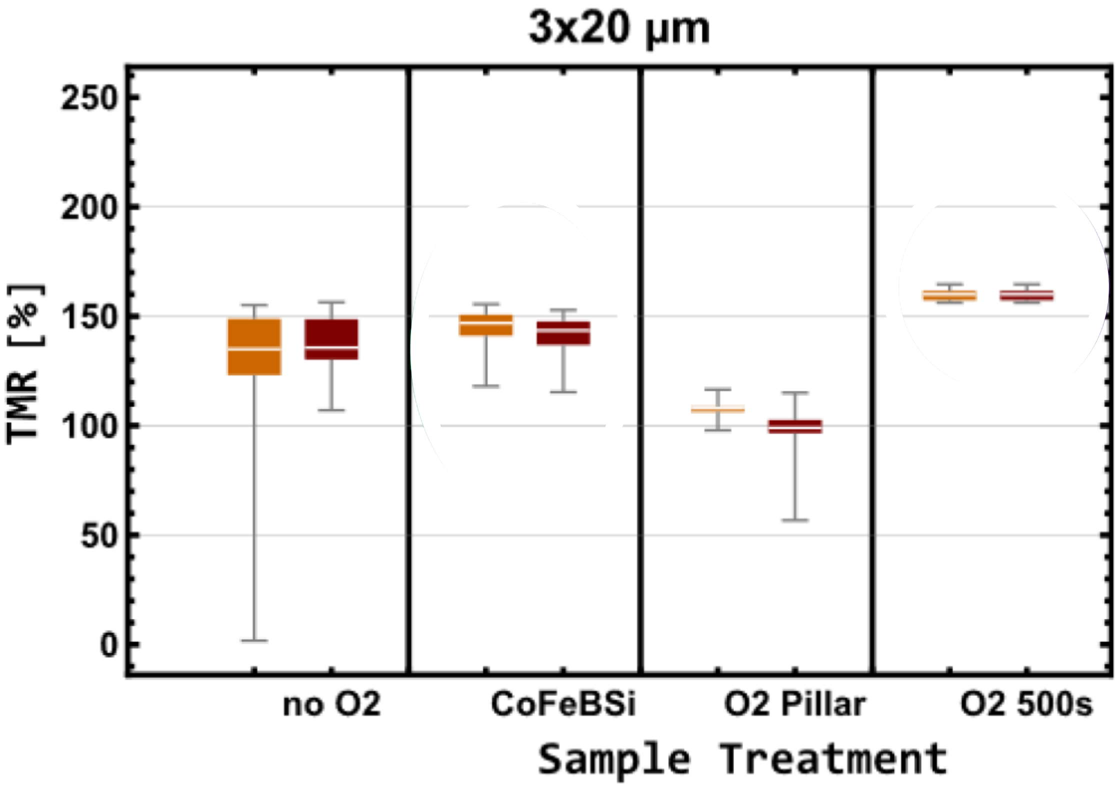

Filipe Monteiro, INESC-MN/IST, Master thesis 2023 (unpublished)

GMR biosensor qualification (6 inch wafers)

INESC MN
Microsistemas & Nanotecnologias

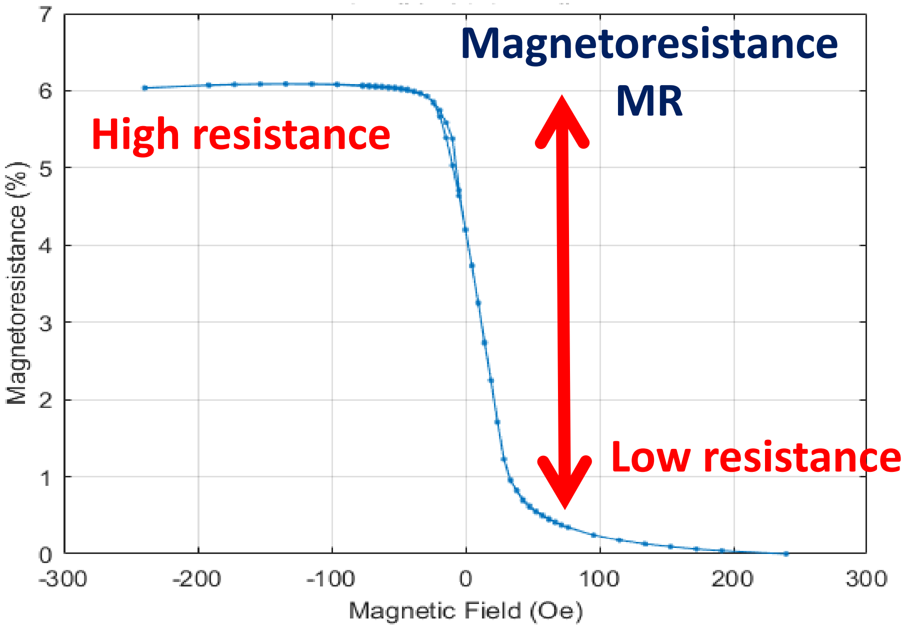

Magnetoresistance (%)
Mean = 6.26 %
Std = 0.97%

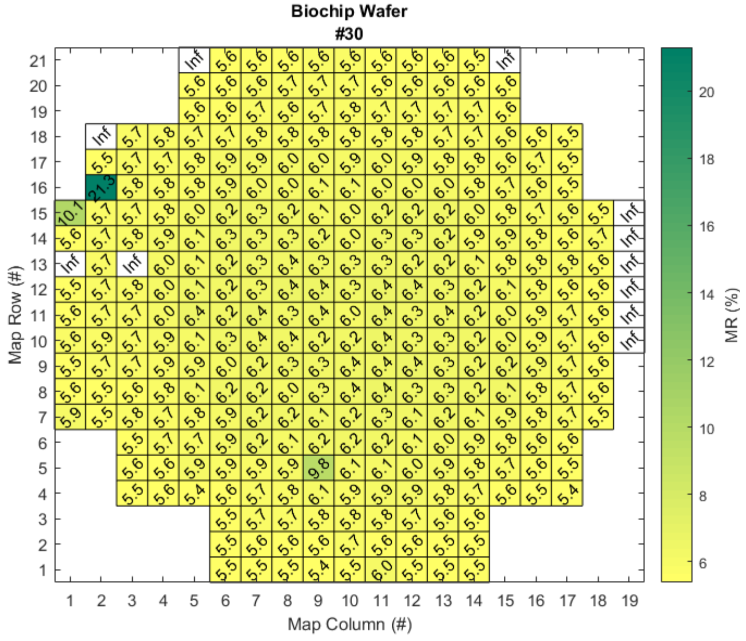

Minimum Resistance (Ω)
Mean = 743.1 Ω
Std = 38.2 Ω

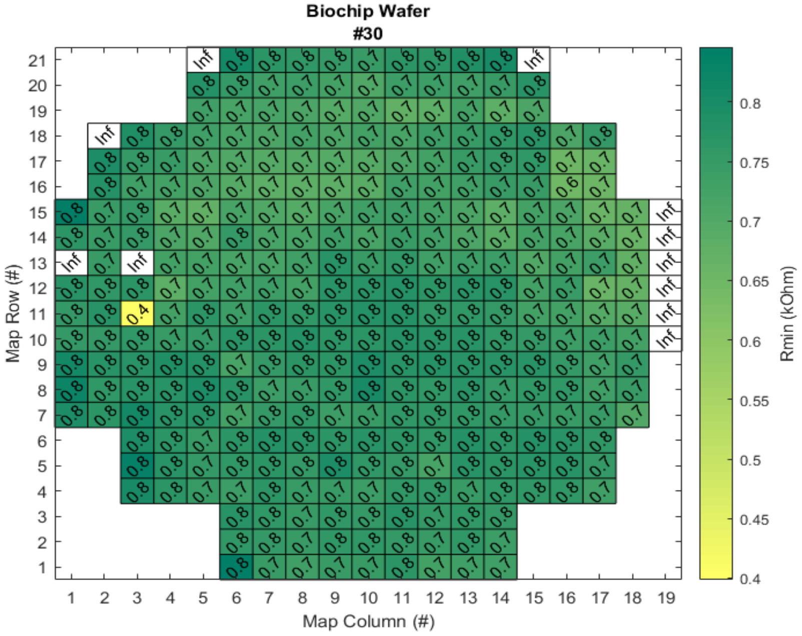

Challenges

- Low fields detection
- Small footprint

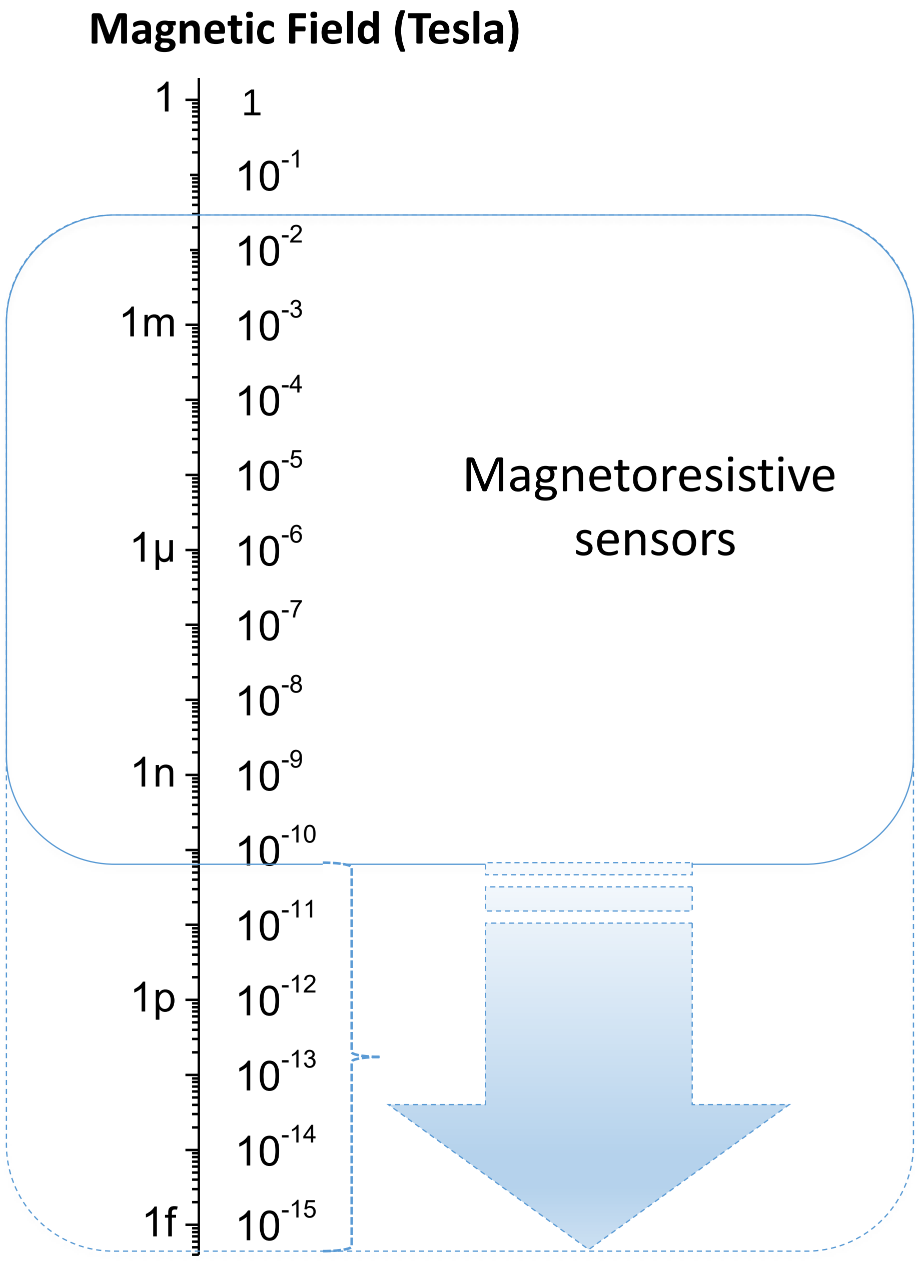

INESC MN
Microsistemas & Nanotecnologias

How to distinguish signal from noise ?

INESC MN
Microsistemas & Nanotecnologias

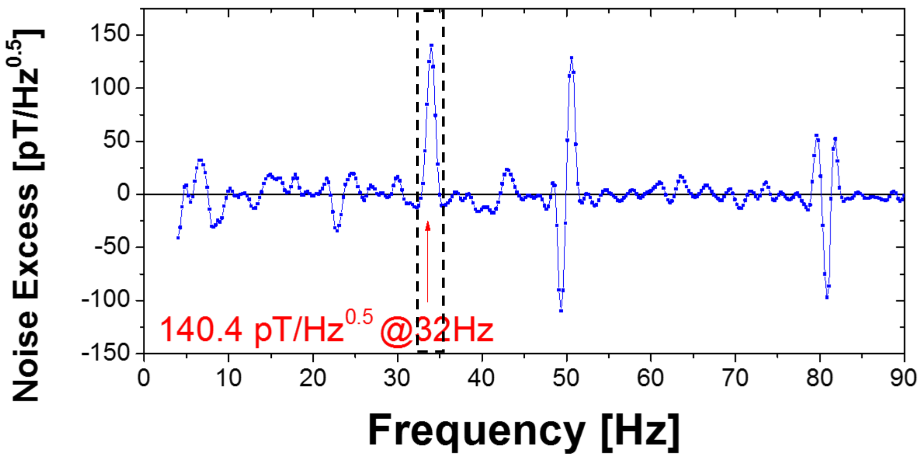

Current I1

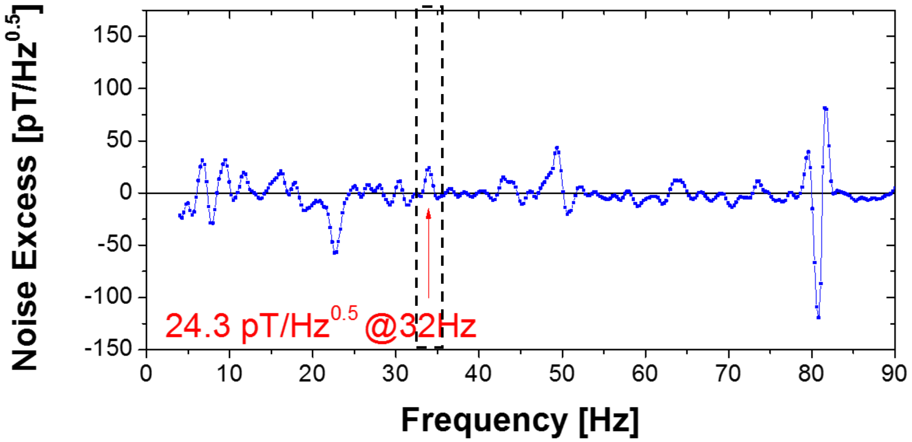

Current I2 < I1

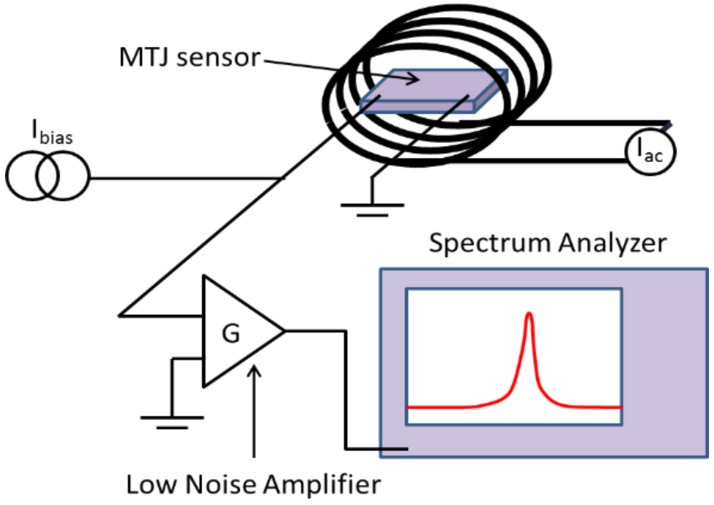

Detectivity limit:

SNR = 1

(Signal = Noise)

P.P.Freitas, R.Ferreira and S.Cardoso "Spintronic Sensors", **Proceedings of the IEEE**, 104, 1894 (2016)

E. Paz · S. Serrano-Guisan · R. Ferreira · P. P. Freitas – J. of Applied Physics; 115. 2014

Noise Spectrum of Magnetoresistive Sensors

Low f + low field

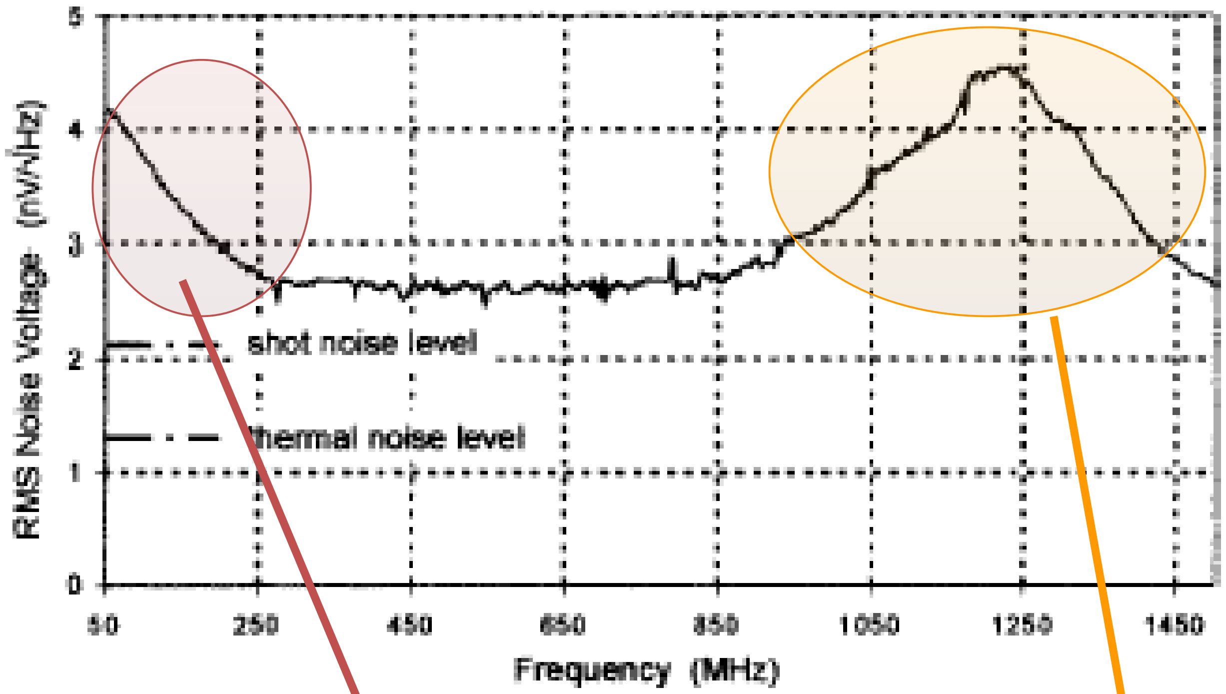

$$S_V(V^2/Hz) = \frac{\alpha_H I^2 R^2}{Af\ \Delta f} + \frac{4K_B TR}{\Delta f} + \frac{2eIR^2}{\Delta f} + FMR_{Noise}$$

1/f noise

Thermal Noise

Shot Noise

High-Frequency Noise

MRI
- 1 T
- 1 mT
Earth field
- 1 µT
- 1 nT
Heart
- 1 pT
Brain
- 1 fT

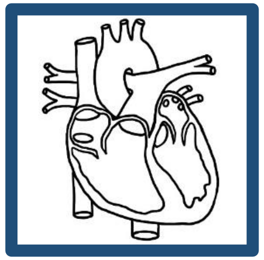

Amplitude:
few **pTesla** at chest surface
(below 100 Hz)

Amplitude:
few **fTesla** at skull surface
(below 100 Hz)

Field detectivity (D)

INESC MN
Microsistemas & Nanotecnologias

Detectivity limit: **SNR = 1** (Signal = Noise)

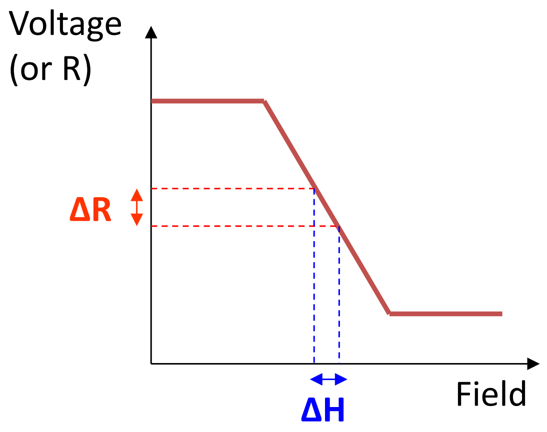

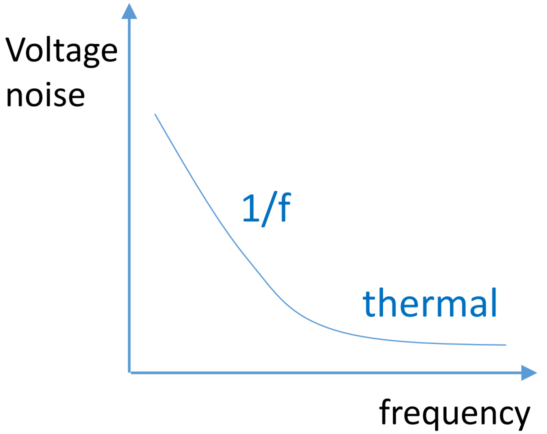

$$S_V\left(T/\sqrt{Hz}\right)=\frac{\sqrt{\dfrac{\alpha_H I^2 R^2}{A\ f}}}{I.\dfrac{\Delta R}{\Delta H}}=\frac{\Delta H}{MR}\sqrt{\frac{\alpha_H}{A\ f}}$$ *[in Tesla]*

(in 1/f regime)

Operate at high f
Increase MR
Increase A
Reduce linear range ΔH
Reduce Hooge value

S=TMR/ΔH
sensor sensitivity

α_H = Hooge's constant
A = MR area
f = operating frequency

Strategies to improve the minimum detectable field

(in 1/f regime)

$$S_V\left(T/\sqrt{Hz}\right)=\frac{\sqrt{\dfrac{\alpha_H I^2 R^2}{V\ f}}}{I.\dfrac{\Delta R}{\Delta H}}=\frac{\Delta H}{MR}\sqrt{\frac{\alpha_H}{V\ f}}$$

[in Tesla]

α_H = Hooge's constant
A = MR area
f = operating frequency

→

Field modulation for high frequency
Increase TMR
Increase V (area or thickness)
Reduce linear range ΔH
Reduce Hooge value

Improve MR

Nat Mater, 2004, 3:862–867
J PhysD-Appl Phys, 2007, 40: R337
J. Physics: Cond.Matter, 19 (2007) 165221
Ann Rev Mater Res, 2009, 39: 277–296
J Appl Phys, 2007, 101: 09B501
J. Appl. Phys, 99, 08A907 2006

Increase A

APL, 91, 102504 (2017)
JAP; 115. 2014
AIP Advances 8(5):056644 (2018)
Scientific Reports , 11, 215 (2021)
IEEE Trans. Magn. **48**, 4111 (2012)

Field modulation

Sensors, *18*(3), 790; (2018)
Micromachines, *7*(5), 88 (2016)
IEEE Trans. Magn. 48 (11), pp. 4115 (2012)
Journal of SPIN, Vol.1 (1), pp 71-91 (2011)
J.Appl.Phys. 103, 07E924 (2008)
Appl. Phys. Lett. 95, 023502 (2009)

Reduce α_H

IEEE Trans. Magn. 51, 1 (2015)
IEEE Trans. Magn. 50, 1 (2014)
Microsys. Technol. 20, 793 (2014)

Reduce linear range

IEEE Trans. Magn. 48 (11), pp. 3847 (2012)
J.Appl.Phys.109, pp.07E521 (2011)
IEEE Trans Magn. 50 (11), 4003805 (2017)
IEEE Trans Magn. 55, 7, 4400605 (2019);

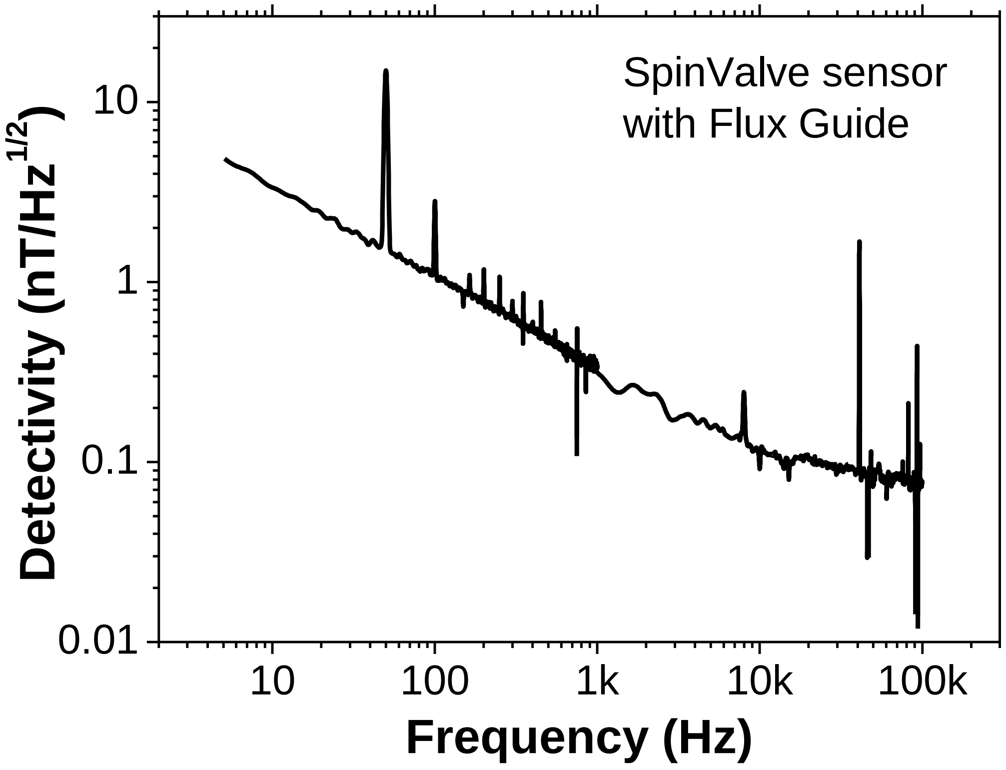

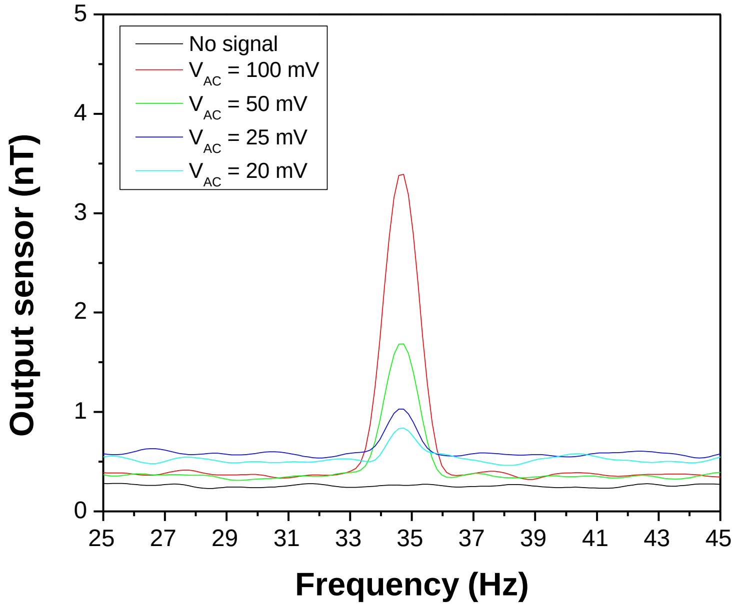

Detectivity values:

3.3 nT/Hz$^{1/2}$ @ 10 Hz
1.9 nT/Hz$^{1/2}$ @ 30 Hz
310 pT/Hz$^{1/2}$ @ 1 kHz

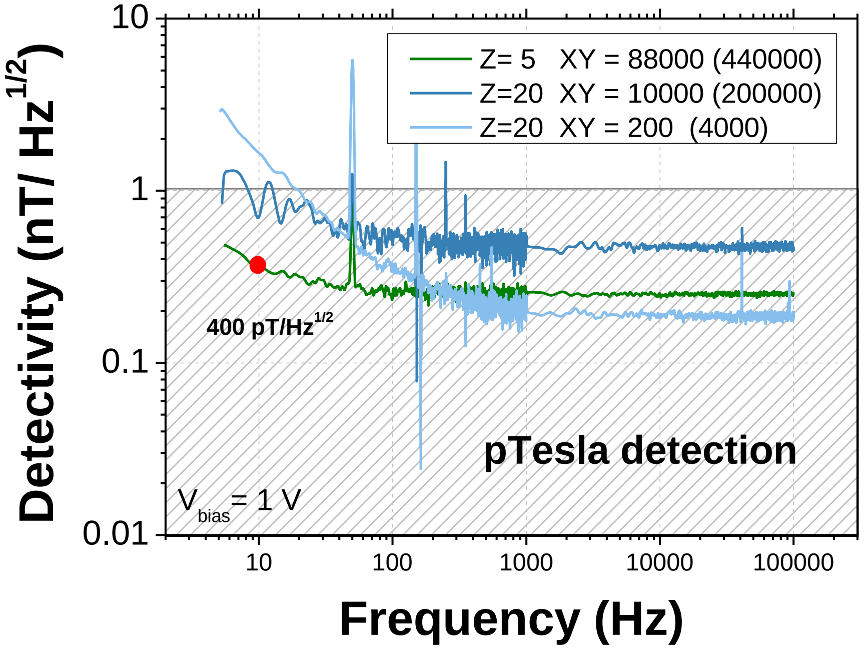

AIP Advances 8(5):056644 (2018)
Scientific Reports , 11, 215 (2021)

Detectivity (D) - **minimum detectable field**

SNR =1

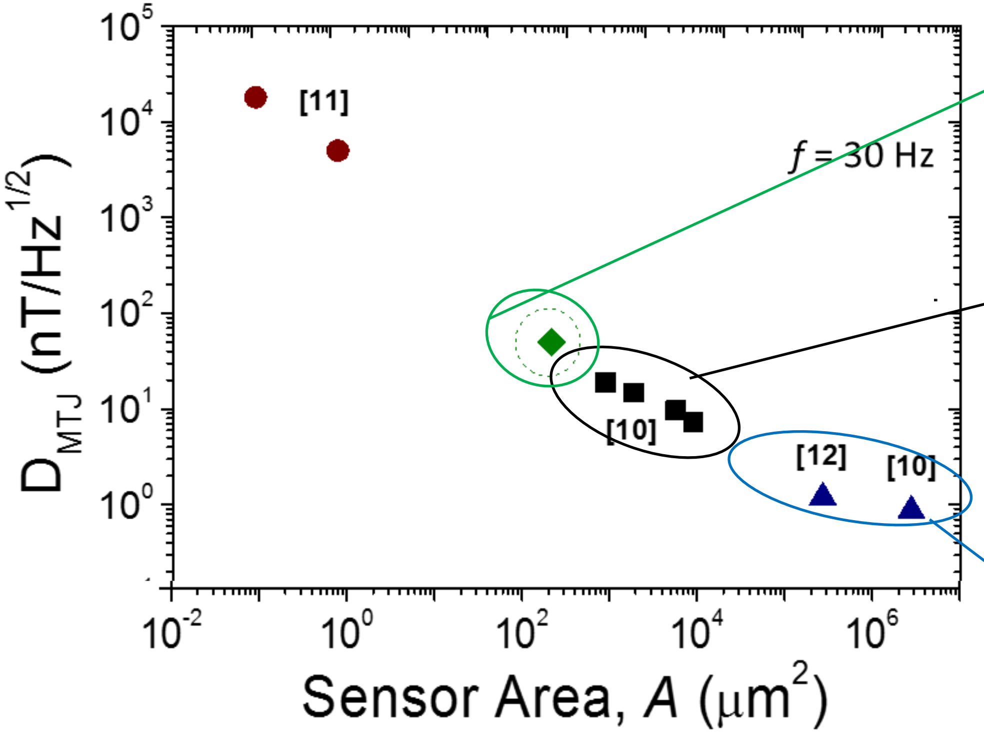

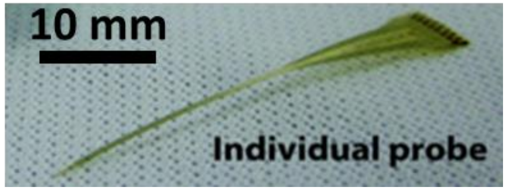

flexible probe - polyimide

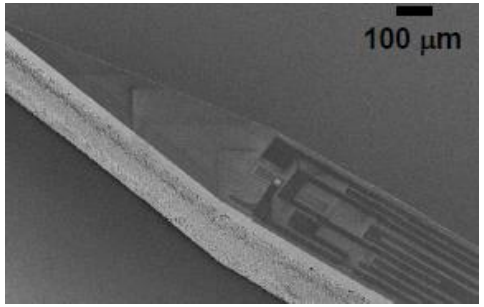

Si probe (single MR)

Si probe (arrays MR)

MAGNETRODES

IEEE Trans Magn. vol. 51 (11) 4401104 (2015) **Neuron,** 95, 1–9 (2017)

J.Gaspar et.al, IEEE Trans Magn. Vol.53 (4), 5300204 (2017

INESC MN
Microsistemas & Nanotecnologias

Large Series
1102 TMR elements with A= 100x100 μm² each.

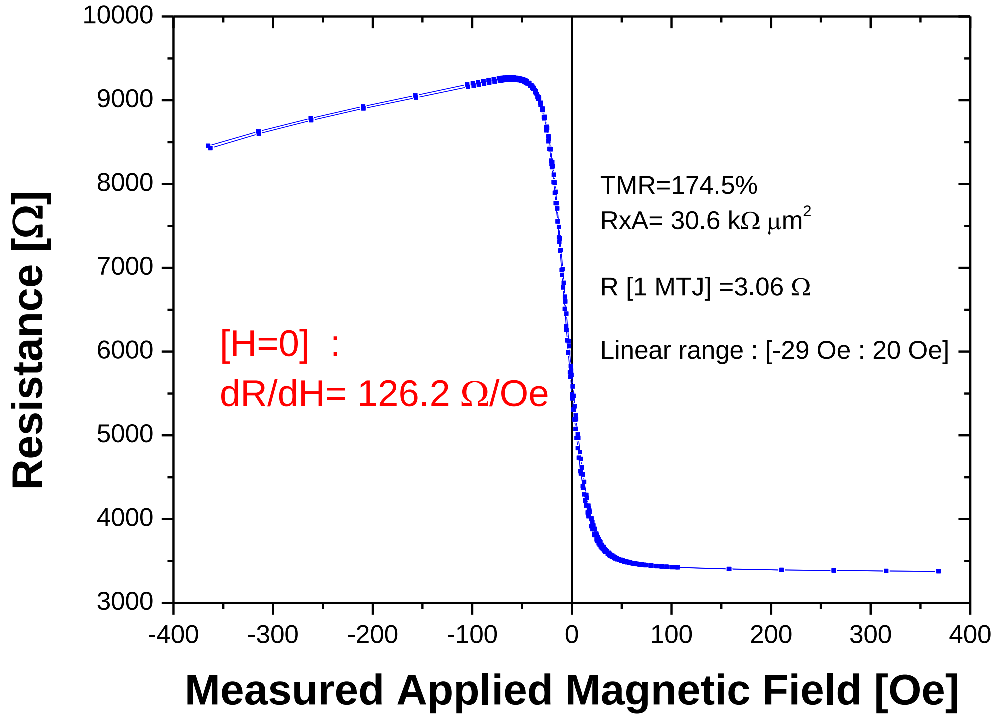

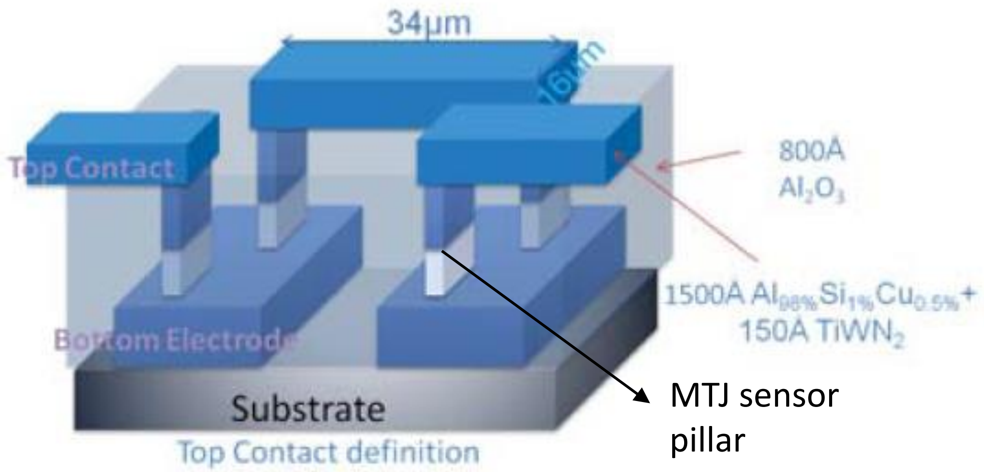

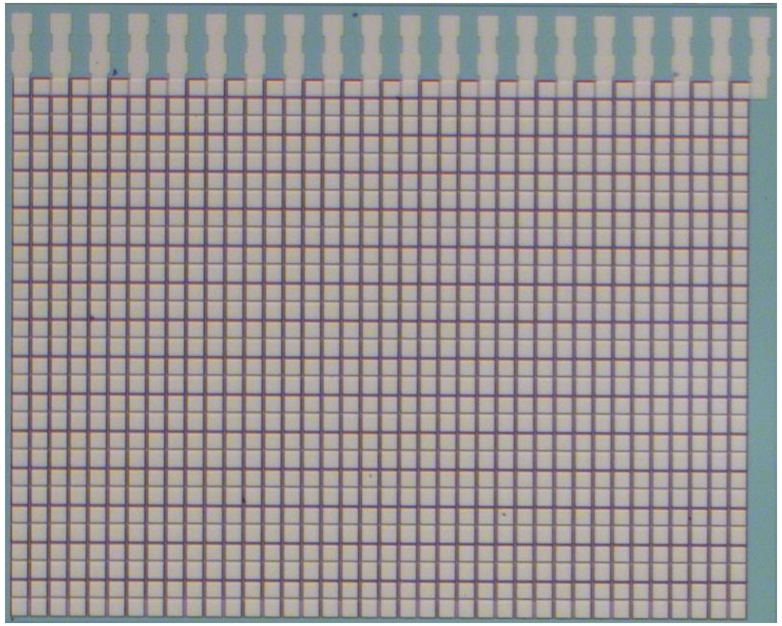

E. Paz · S. Serrano-Guisan · R. Ferreira · P. P. Freitas - Journal of Applied Physics; 115. 2014

Increase V (area or thickness)

INESC MN
Microsistemas & Nanotecnologias

...for people with enough space

...for all others

Courtesy: C.Caldeira, Nanium

Saving space: GMR sensors packed

Single sensor

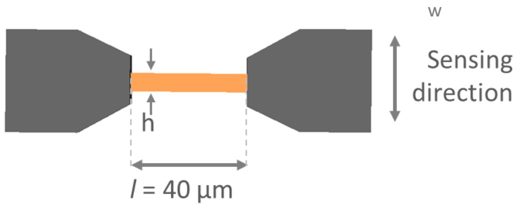

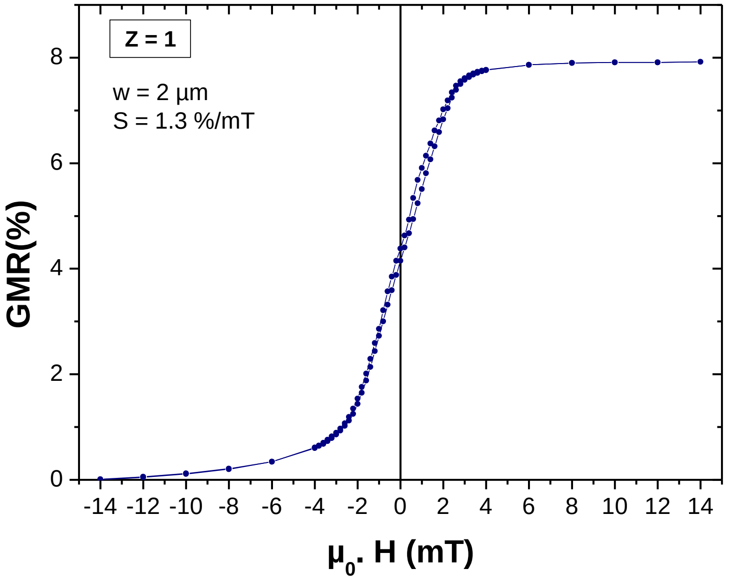

Packed sensors

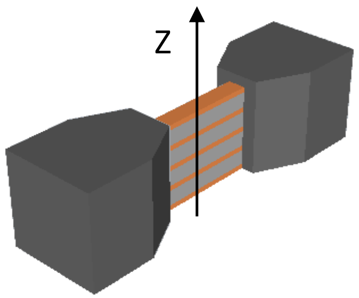

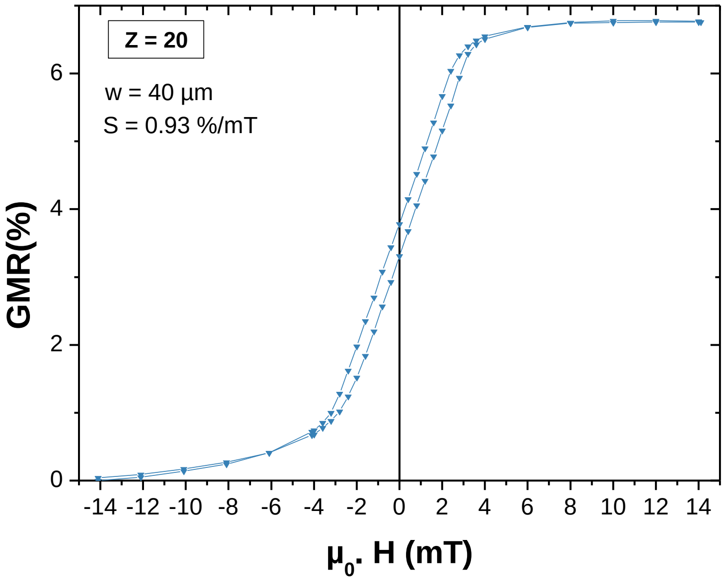

Packed arrays of sensors

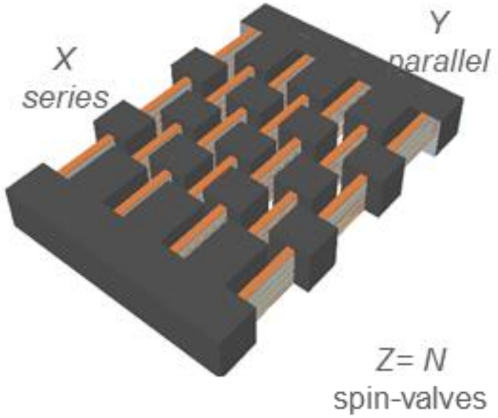

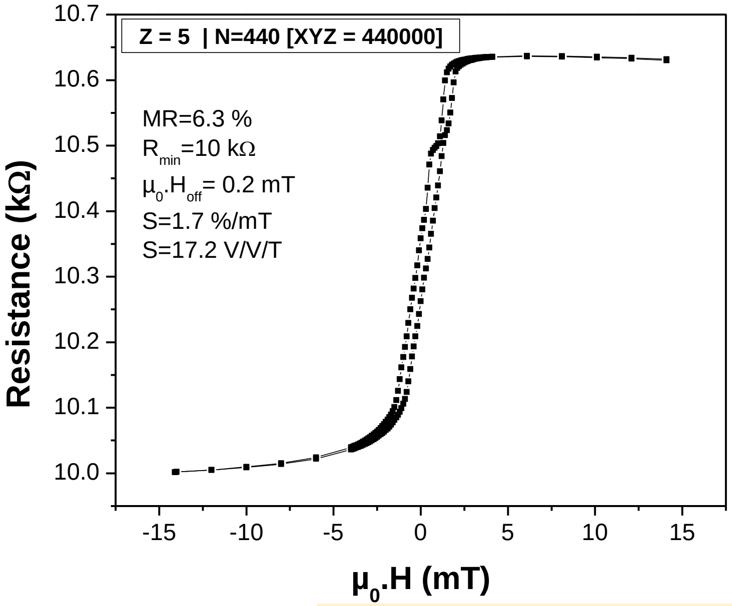

AIP Advances 8(5):056644 (2018)
Scientific Reports , 11, 215 (2021)

TMR sensors packed

TMR structure

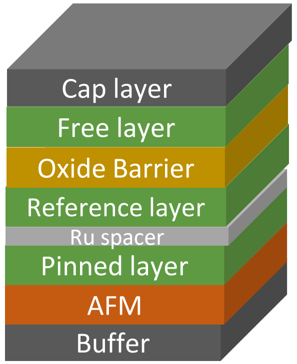

a) Vertical Packed single MTJ

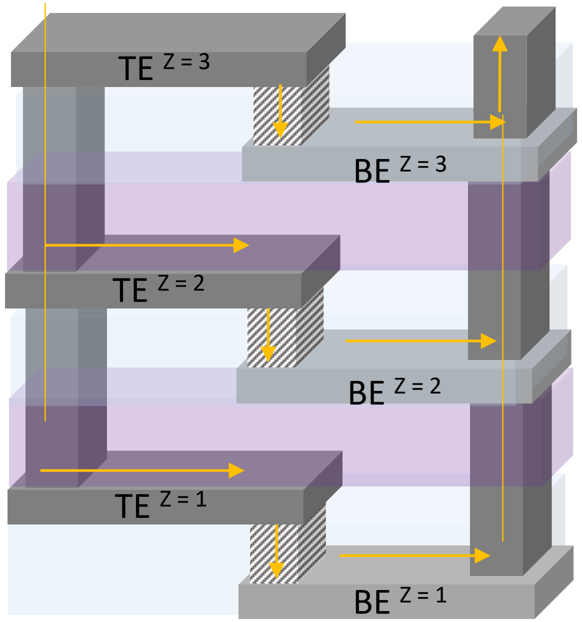

b) Vertical Packed MTJ Array

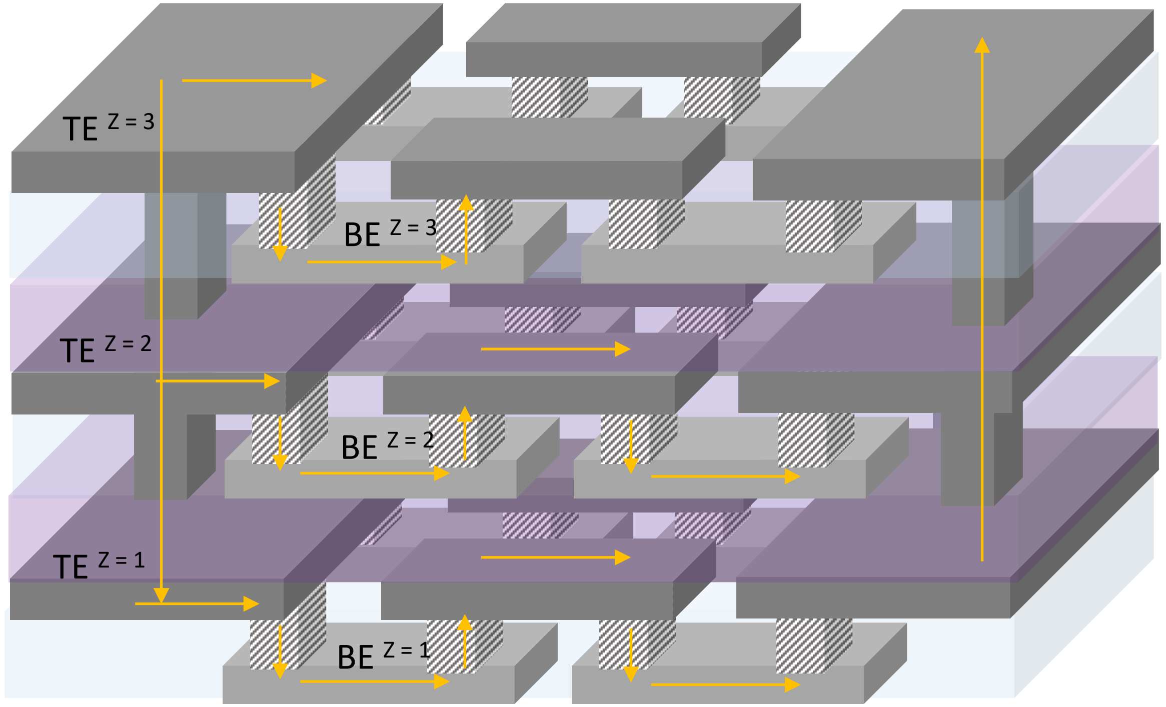

INESC MN
Microsistemas & Nanotecnologias

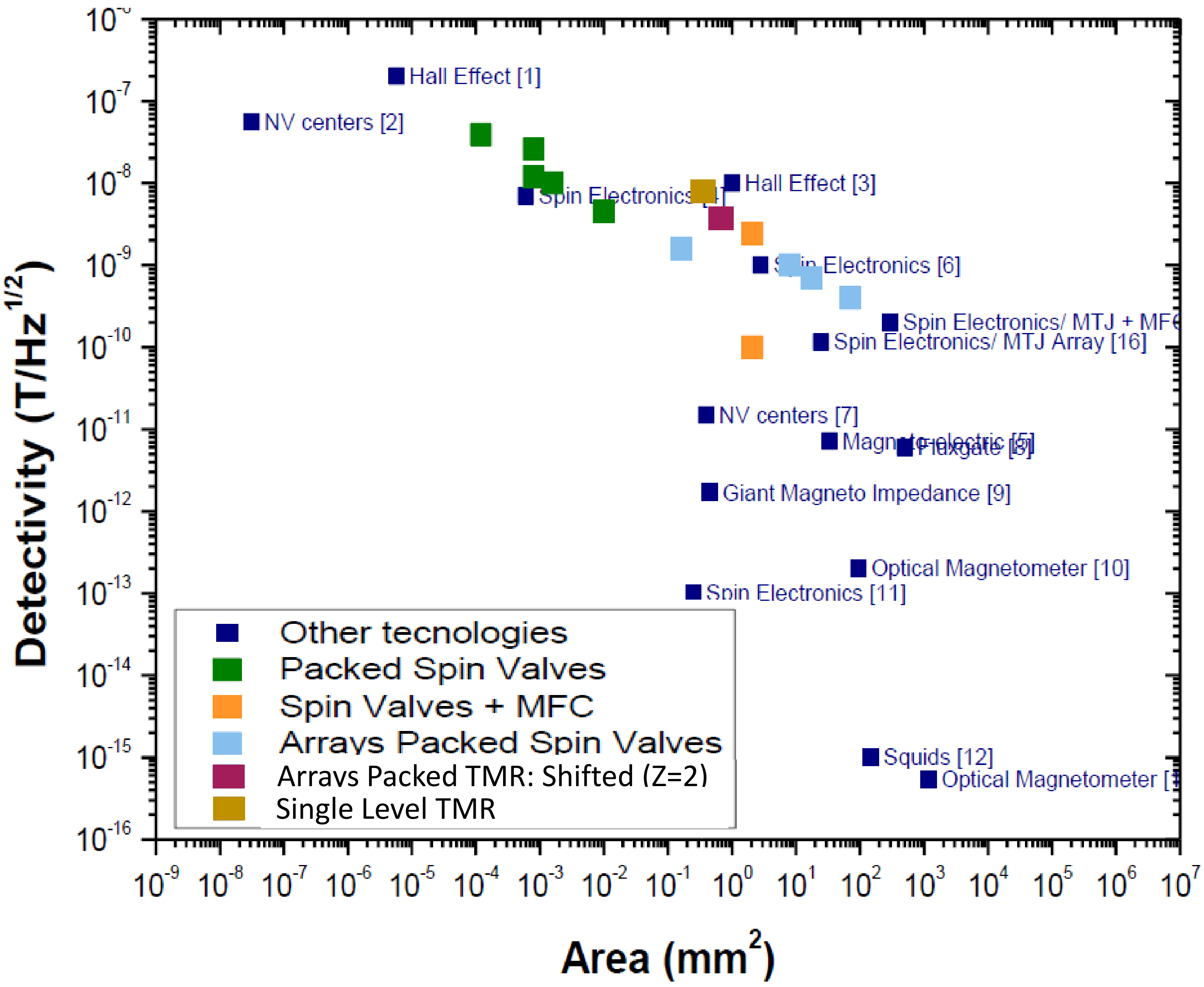

AIP Advances 8(5):056644 (2018)
Scientific Reports , 11, 215 (2021)

[1] E. Paz et al., *J. Appl. Phys.*, vol. 115,2014.
[2] tdk.com, “TDK biomagnetic sensor”, 2019
[3] S. H. Liou *et al.*, *Proc. IEEE Sensors*, 2009

[1] P. Besse *et al* Appl. Phys. Lett. **80**, 4199 (2002)
[2] P. Maletinsky et al Nature Nanotechnology 7, 320-324 (2012)
[3] F. Montaigne et al Sensors and Actuators A: Physical 81, 324-327 (2000)
[4] L. Caruso et al Neuron 95, 1283-1291 (2017)
[5] R. Jahns et al Sensors and Actuators A: Physical 183, 16-21 (2012)
[6] F. Barbieri et al Scientific Reports 6, 39330 (2016)
[7] J. Barry et al PNAS 113, 14133-14138 (2016)
[8] Bartington Instruments, Mag-03 Three-axis
[9] S. Yabukami et al JMMM 290, 1318-1321 (2005)
[10] T. Sander et al Biomedical Optics Express 3, 981-990 (2012)
[11] M. Pannetier et al Science 304, 1648-1650 (2004)
[12] J. Gallop Supercond. Sci. Technol. 16, 1575 (2003)
[13] I. Kominis et al Nature 422, 596-599 (2003)
[14] E. Paz et al., *J. Appl. Phys.*, vol. 115,2014.
[15] tdk.com, “TDK biomagnetic sensor”, 2019
[16] S. H. Liou *et al.*, *Proc. IEEE Sensors*, 2009

Challenges II

- Wheatstone Bridge architecture
- Thermal stability

If no more time:
press to end

CHALLENGE: WHEATSTONE BRIDGE

INESC MN
Microsistemas & Nanotecnologias

TMR sensor acts as a variable resistor

Simplest way to measure:

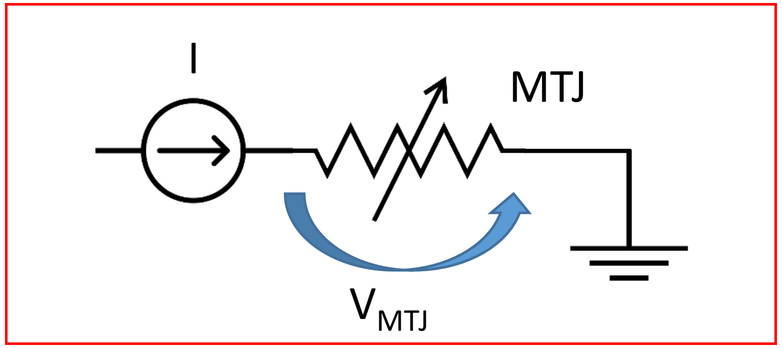

Disadvantages:
- Current source is difficult to implement
- Prone to supply noise
- Output is not zero when field is zero

Wheatstone bridge

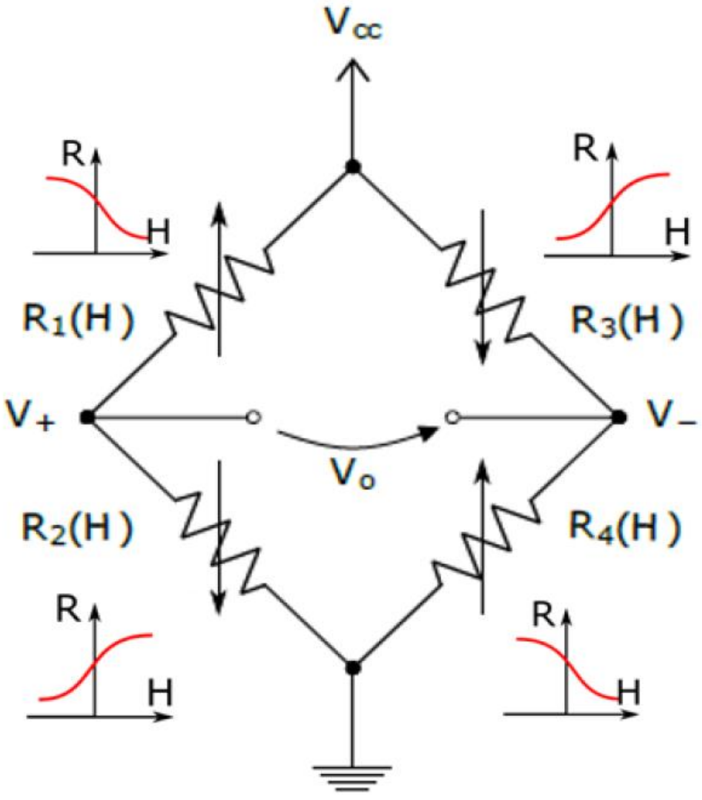

$$V_o = \left(\frac{R_2(H)}{R_1(H) + R_2(H)} - \frac{R_4(H)}{R_3(H) + R_4(H)} \right) V_{cc}$$

Advantages:
- Bipolar output
- Noise immunity
- Easy biasing (V const)

Disadvantage:
- Requires 4 TMR sensors
- **Anti-parallel sensitivities**

↓

2 reference directions for X
2 reference directions for Y
in the same die

Full bridge with mechanical mounting

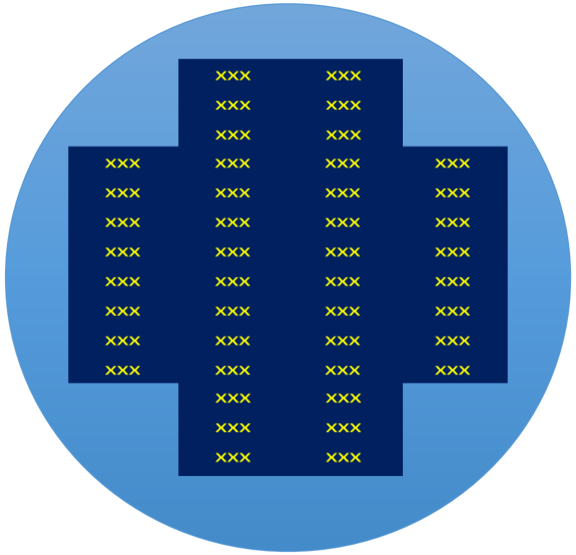

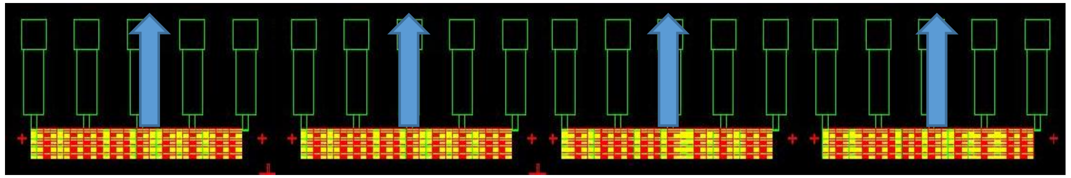

1 deposition step for TMR definition
The same annealing for all wafer

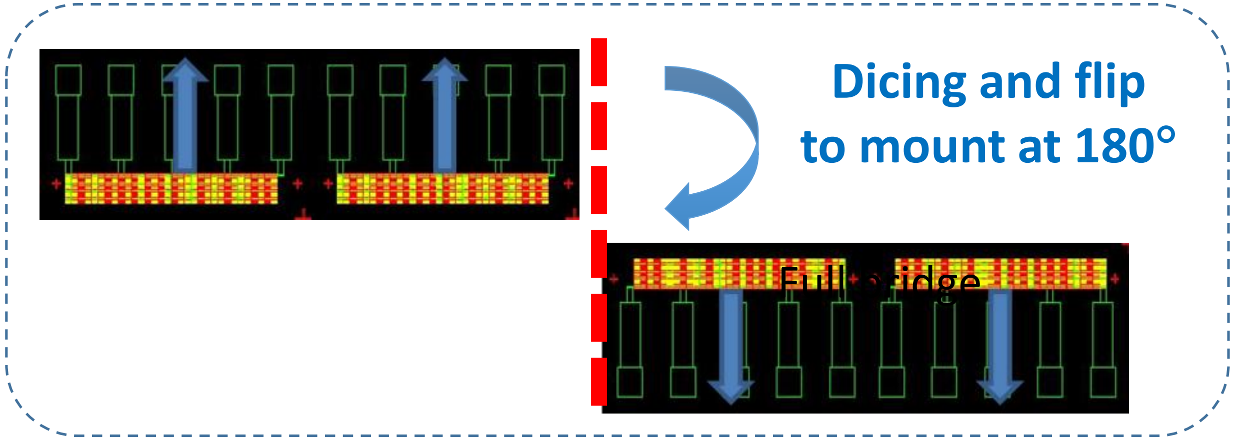

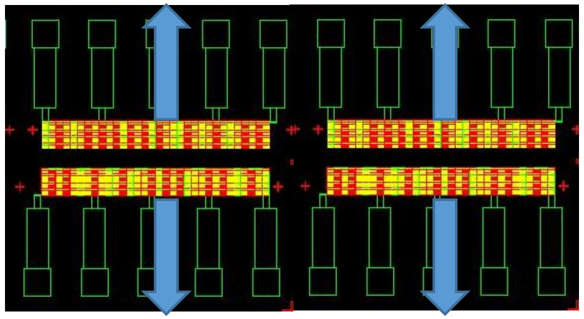

Full Weatstone Bridge

WHEATSTONE BRIDGE – DISCRETE COMPONENT ASSEMBLY

INESC MN
Microsistemas & Nanotecnologias

1 direction

1 deposition

Individual sensors

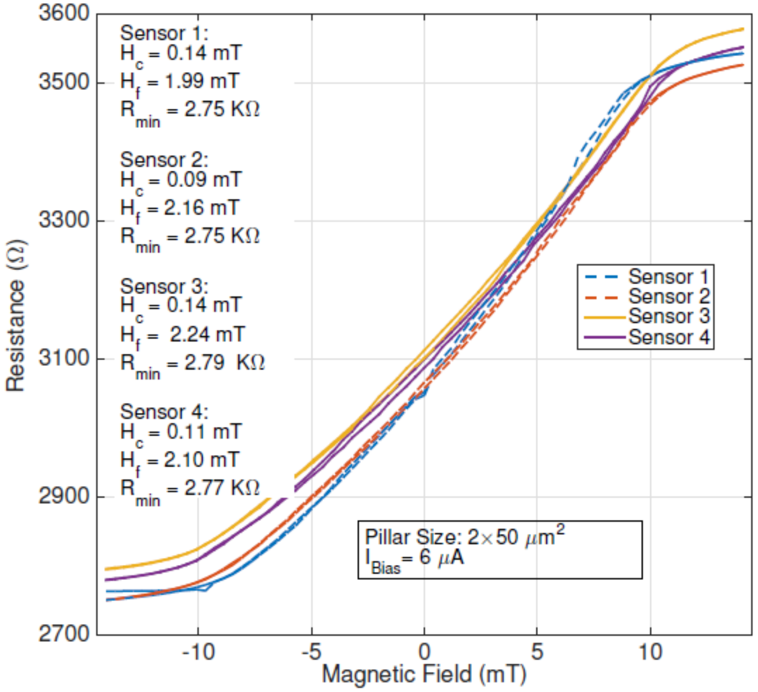

(a) Output of the four sensors that compose the bridge after annealing.

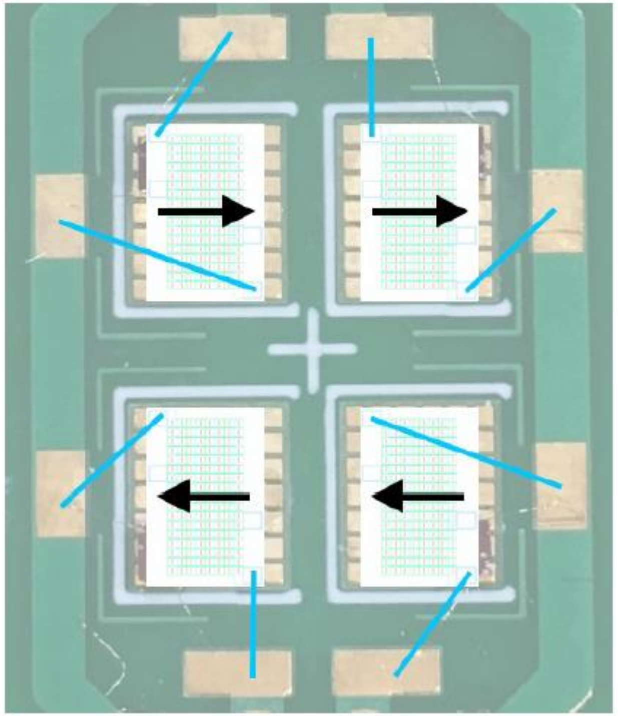

4 AlOx chips mounted in Wheatstone Bridge

Each chip = 225 x (2x50 um²)

1D Wheatstone bridge

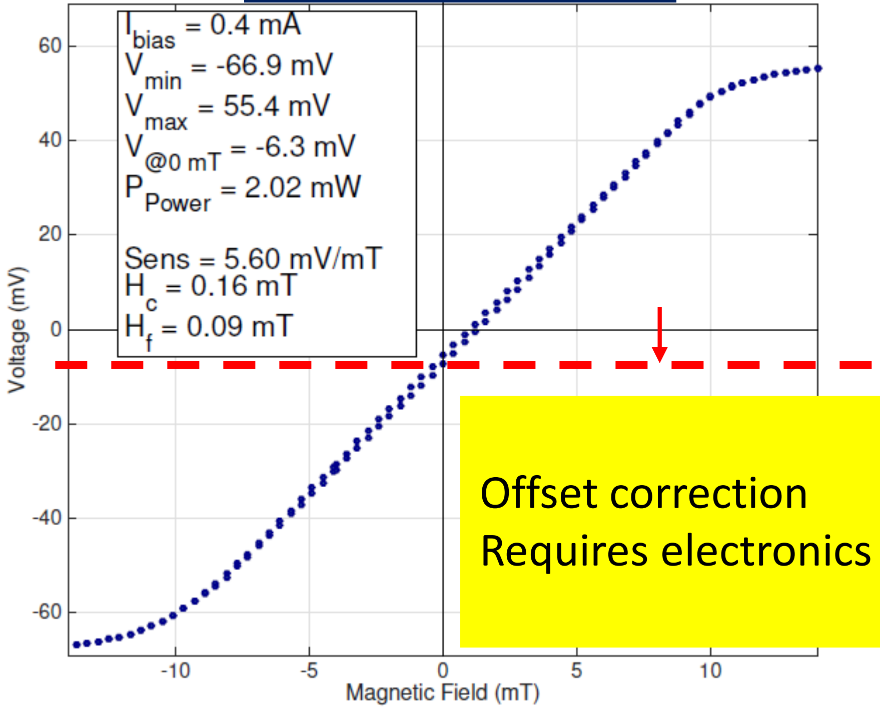

Offset correction
Requires electronics

Full bridge with 2 depositions

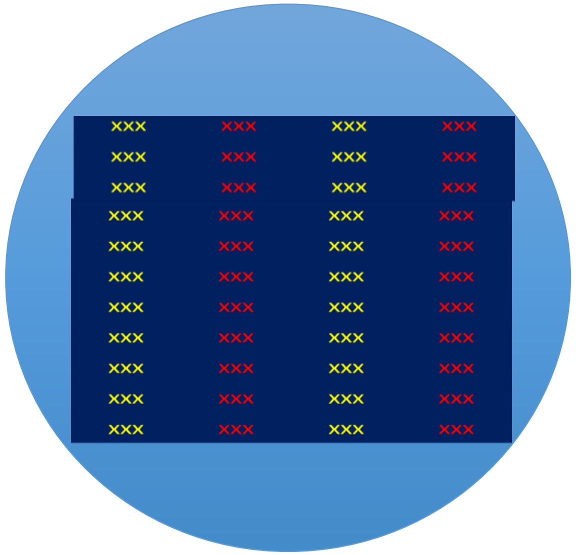

2 deposition steps for TMR definition

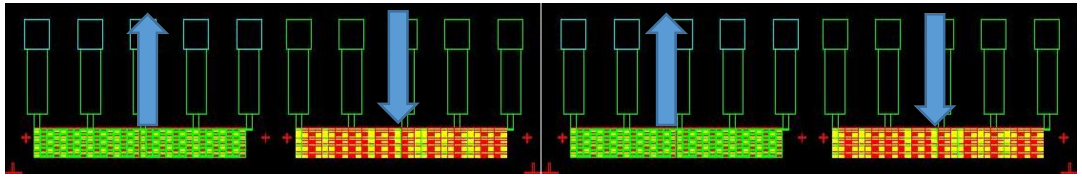

WHEATSTONE BRIDGE – 180° REFERENCE LAYERS

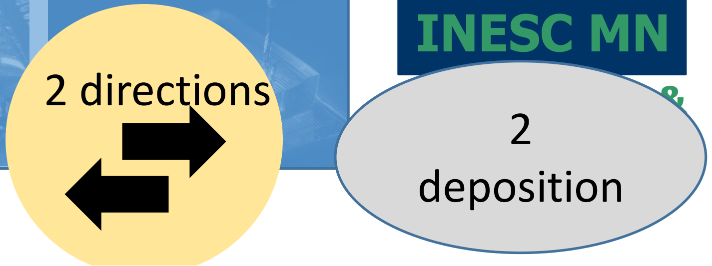

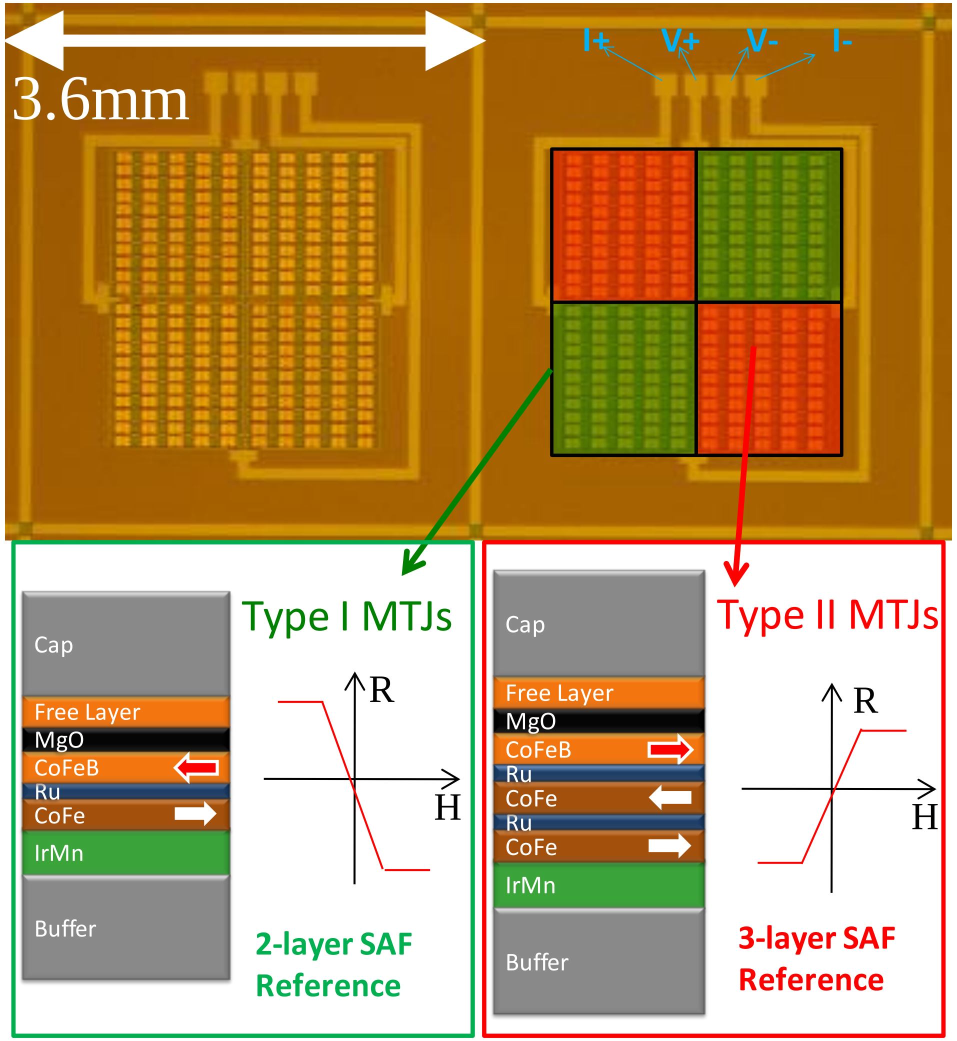

Appl.Phys.Letters 118, 072401 (2021)

IEEE Transactions on Magnetics 48, 4107 (2012)

1D Wheatstone bridge

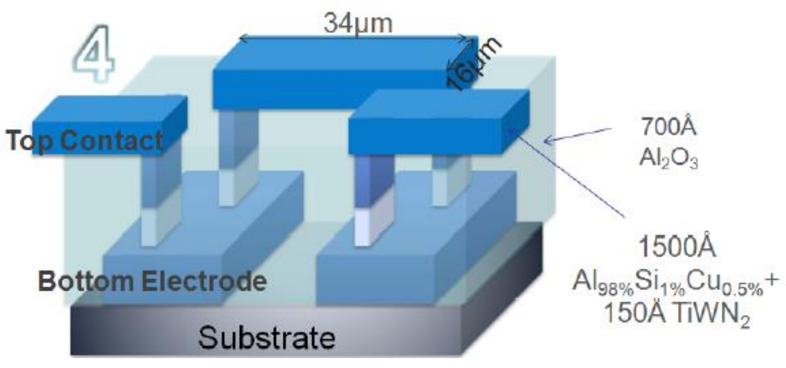

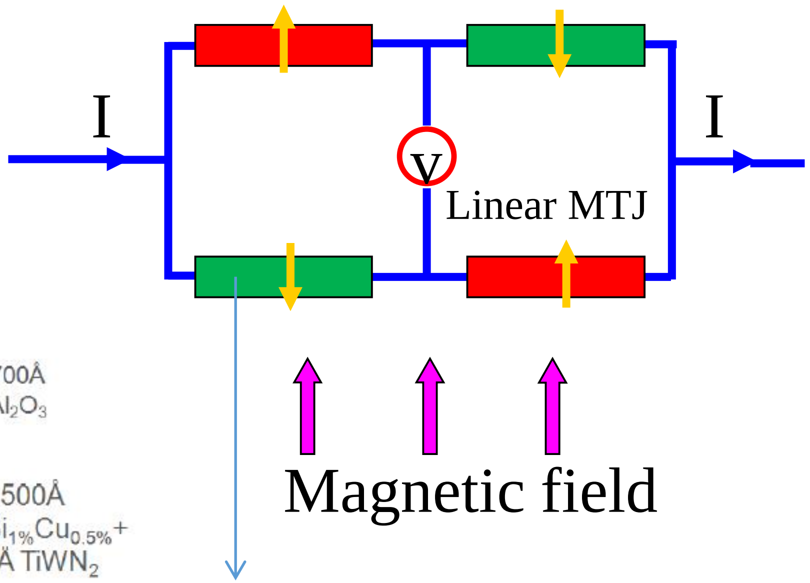

Individual MTJ Area: 5x70 μm^2

MTJ Elements in series: 110 per arm

Annealing at 330ºC required for both TMR stacks at wafer level

Exchange coupling – Hysteresis loop

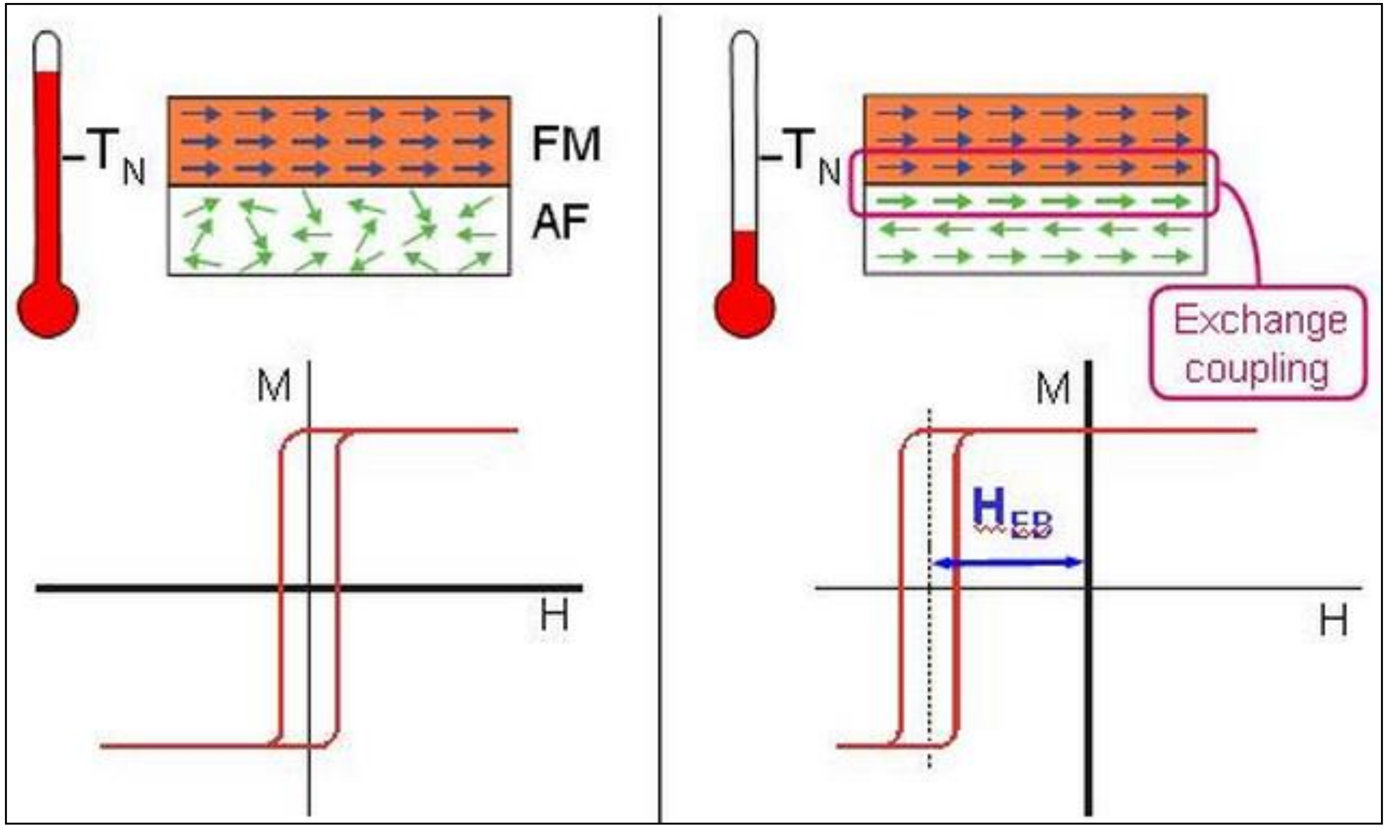

Antiferromagnet:
MnIr, MnPt, MnNi, NiO…

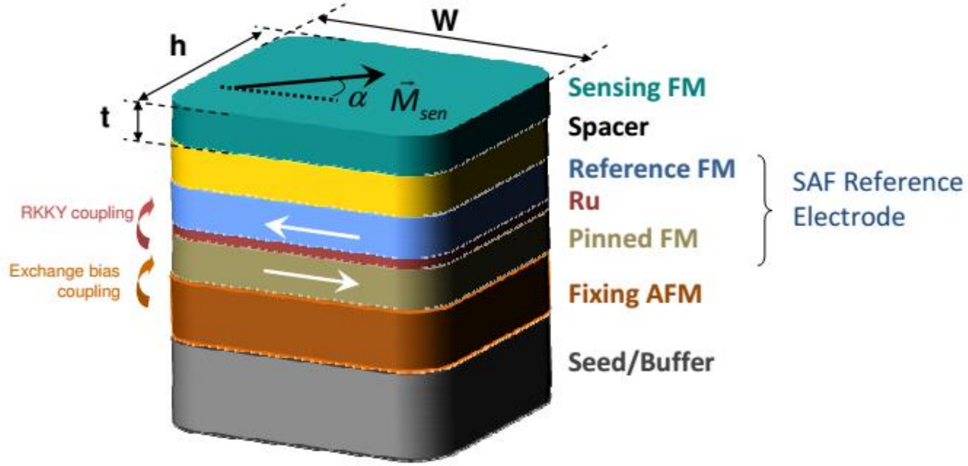

Simple Model

$$E = \frac{1}{2} n J_{ex} S_F S_{AF} + M_F t_F H$$

$$H_b = \frac{n J_{ex} S_F S_{AF}}{2 M_F t_F}$$

n - number of interfacial spins per unit area;
J_{ex} - exchange constant at the interface.

Wafel level laser repining

1
deposition

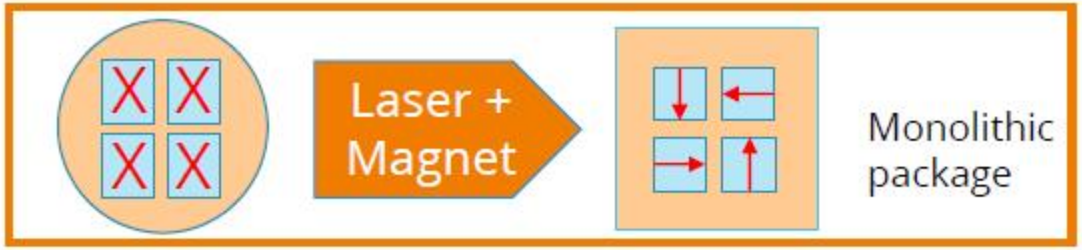

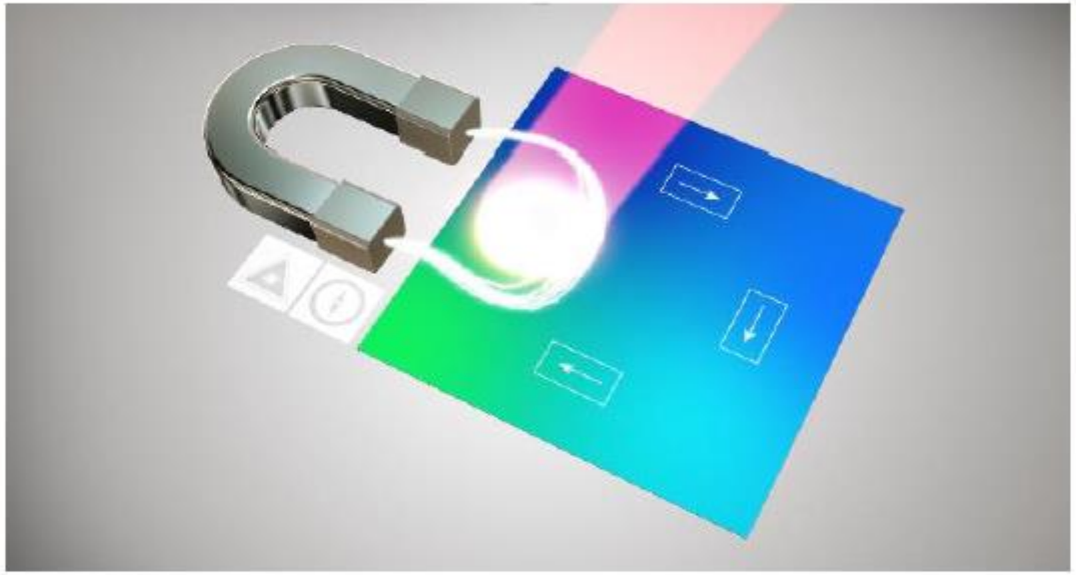

3D MICROMAC

infrared laser λ = 1064 nm
Spot size ~ 10 µm
pulse duration ~100 ns

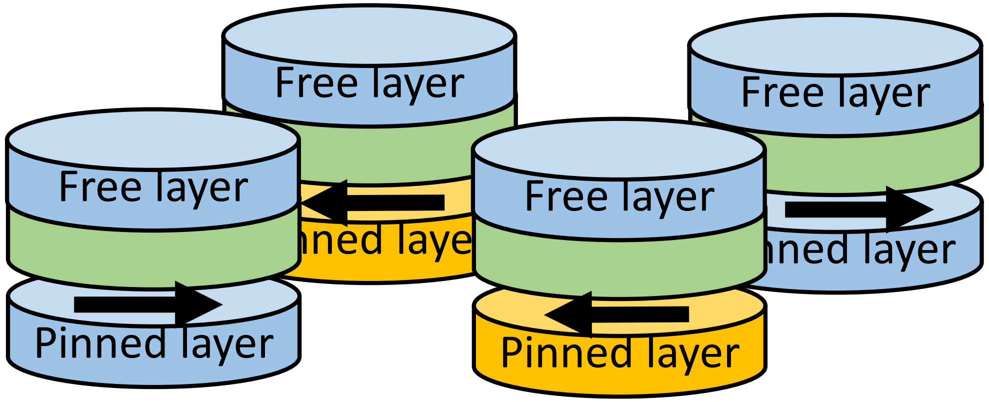

What is the best temperature to reverse the pinned layer?

Sci Rep 11, 14104 (2021).

IEEE Trans. Magn. 51(1) 4002404 (2017)

Appl. Surface Science 302, pp. 159–162 (2014)

Selecting the AF material

INESC MN
Microsistemas & Nanotecnologias

Low T_B → **Easier laser repining**

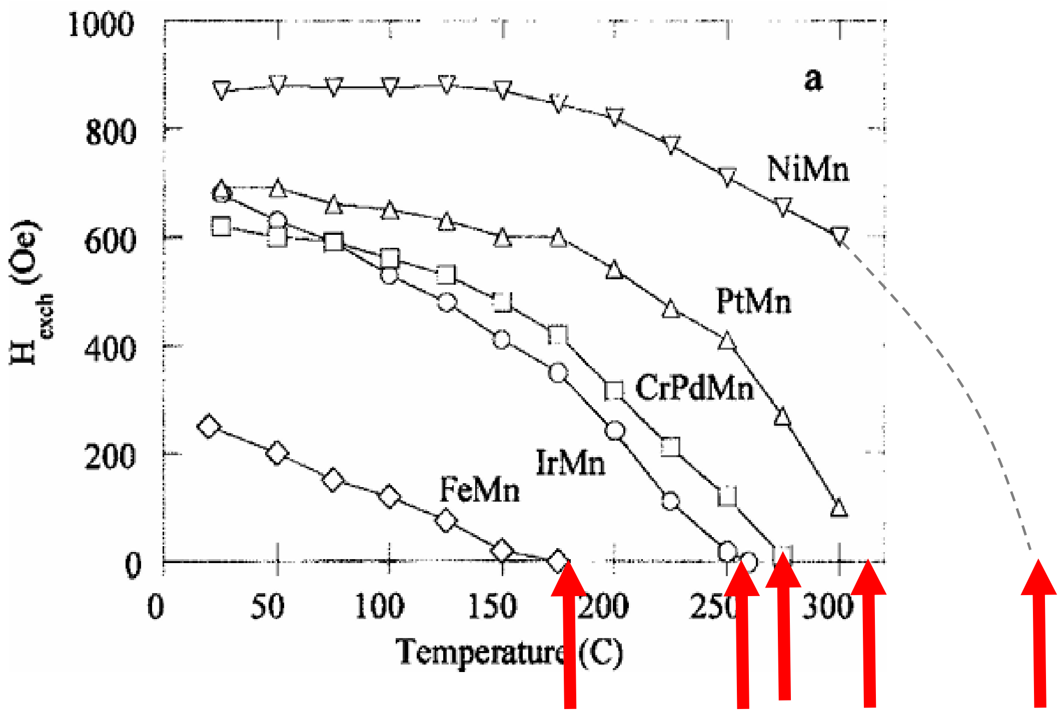

Nozieres et al.
J. Appl. Phys., 87 (8), 15 (2000)

Selecting the repining T for each AF material

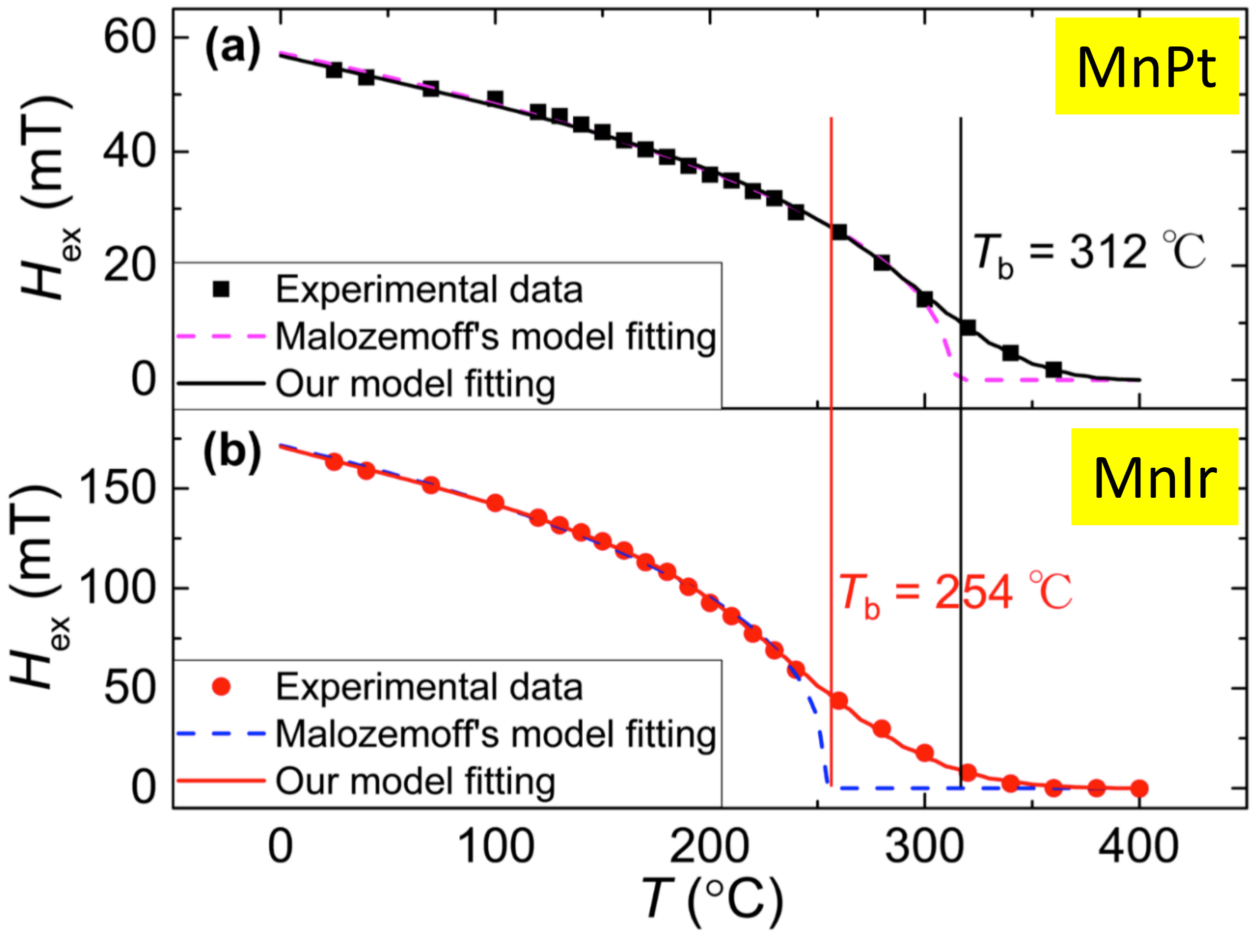

Malozemoff's Model:

$$H_{ex}(T) = \frac{J_{int}^0}{M_{FM}t_{FM}} j(T) = H_{ex}^0 j(T)$$

$$j(T) = \begin{cases} \left(1 - \frac{T}{T_b}\right)^\gamma & : T < T_b \\ 0 & : T \geq T_b \end{cases}$$

Including T_b distribution :

$$H_{ex}(T) = \frac{H_{ex}^0}{1 - \left(\frac{T}{T_c}\right)^{3/2}} \sum_i f\left(T_{bi}\right) \begin{cases} \left(1 - \frac{T}{T_{bi}}\right)^\gamma & : T < T_{bi} \\ 0 & : T \geq T_{bi} \end{cases}$$

$$f\left(T_b^i\right) = \frac{1}{\Delta T_b \sqrt{2\pi}} exp\left[-\frac{\left(T_b^i - T_b^{center}\right)^2}{2\left(\Delta T_b\right)^2}\right]$$

J Magn. Magn. Mater. **477**, 68-75 (2019).

Coercivity, T_B distribution

T_B distribution ➔ uncertainty in laser annealing

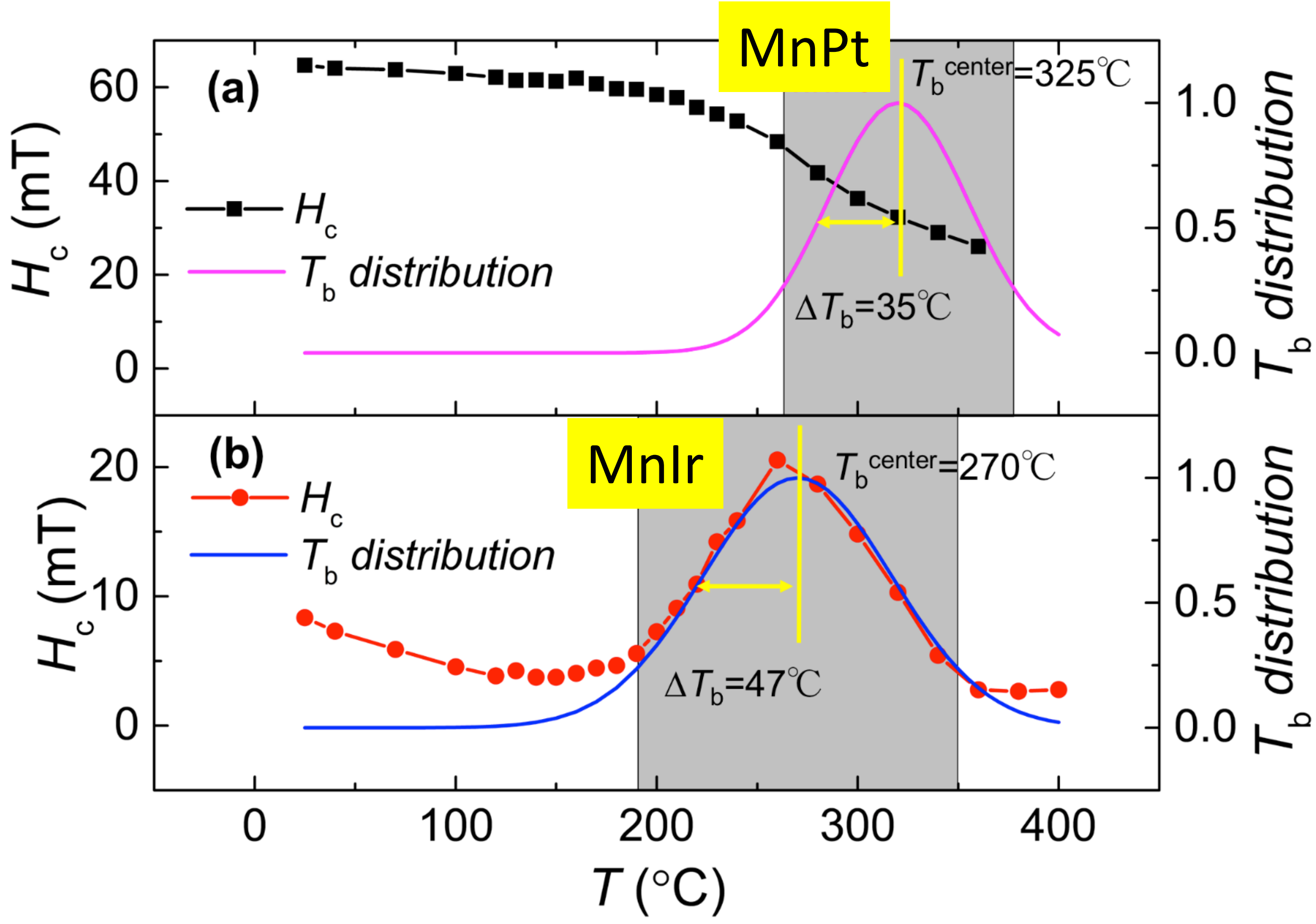

H_c Model: dependency on the grain size

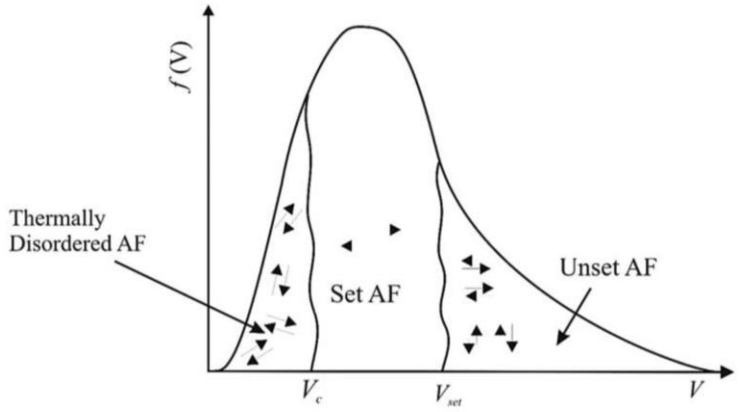

H. Lv *et al.*, *J Magn. Magn. Mater*. **477**, 68-75 (2019).

Selecting the AF material

High T_B → High thermal stability

Nozieres et al.
J. Appl. Phys., 87 (8), 15 (2000)

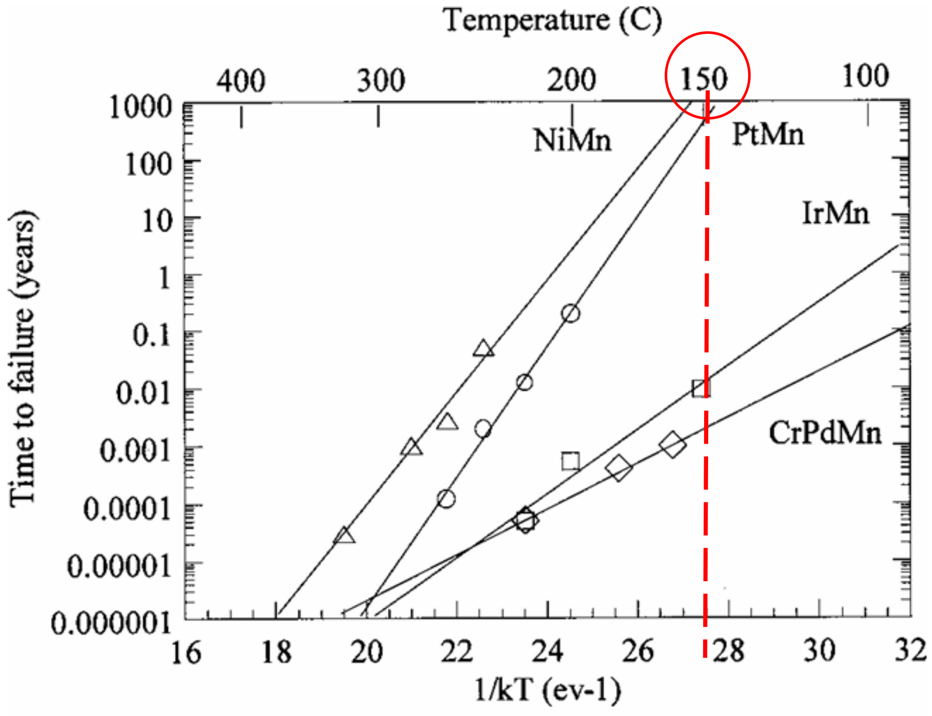

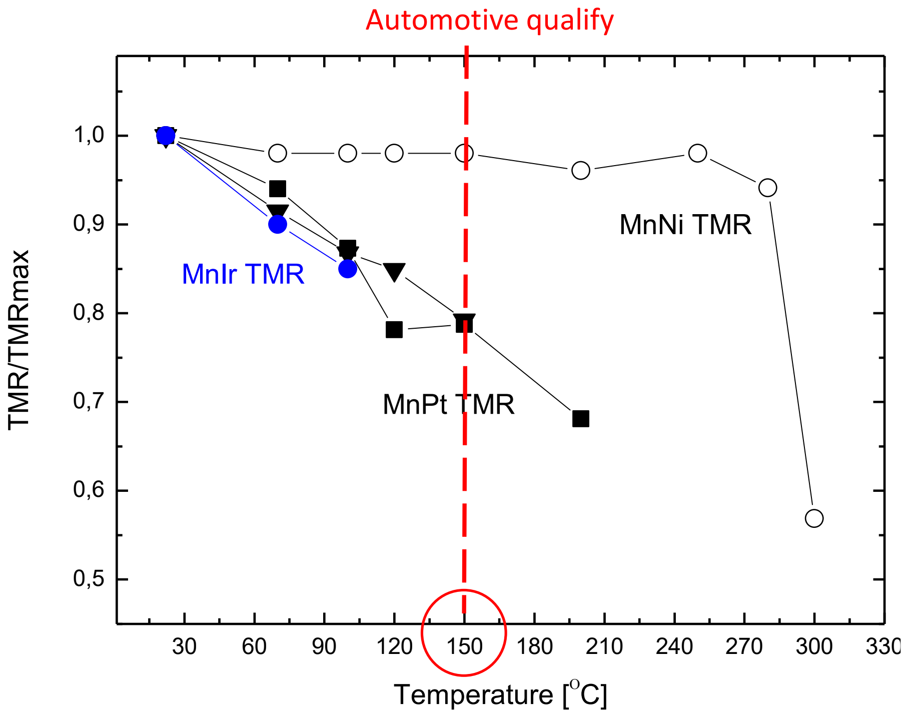

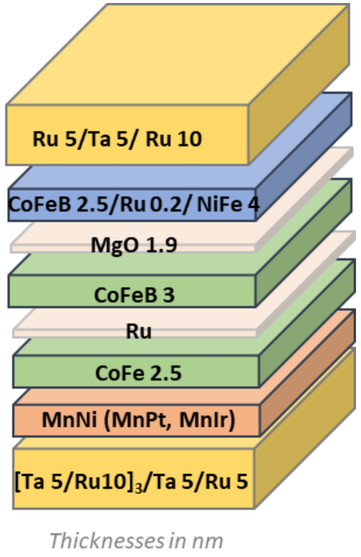

P.Araujo et. al.
(unpublished)

Accelerated annealing tests   At 150°C →

1000 years - NiMn and PtMn
100 days - IrMn
20 h - CrPdMn

In summary:

The perfect magnetoresistive sensor

- large output voltage:	mV
- low field detection:	pT
- tunable for large field detection:	80 mT
- low noise	
- low hysteresis	0 mT
- linearity:	< 1% non-linearity
- small footprint:	10 µm chip size
- low cost:	< 0.20 €/chip
- high thermal stability:	>120°C in harsh e.m environment
- compatible with CMOS modules	
- compatible with large scale microfabrication	
- compatible with flexible electronics	

Is still to be found

Acknowledgments

INESC MN
Microsistemas &
Nanotecnologias

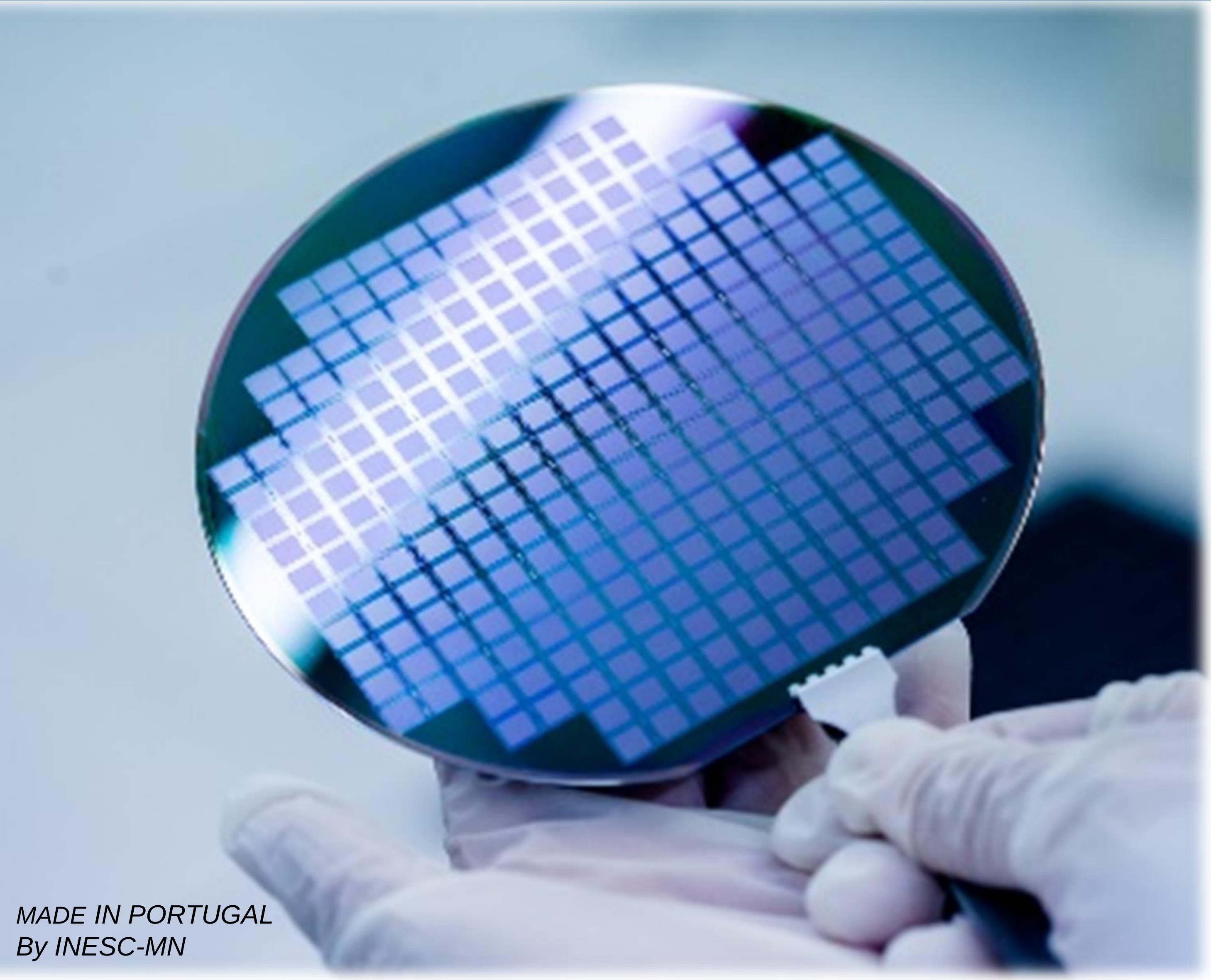

MI MISSÃO INTERFACE

ANI AGÊNCIA NACIONAL DE INOVAÇÃO

REPÚBLICA PORTUGUESA

PRR Plano de Recuperação e Resiliência

Financiado pela União Europeia NextGenerationEU

IAPMEI

fct Fundação para a Ciência e a Tecnologia

nffa.eu research infrastructure

inesc id lisboa

INL INTERNATIONAL IBERIAN NANOTECHNOLOGY LABORATORY